Stratospheric lifetimes of CFC-12, CCl$_4$, CH$_4$, CH$_3$Cl and N$_2$O from measurements made by the Atmospheric Chemistry Experiment-Fourier Transform Spectrometer (ACE-FTS)

A. T. Brown[1], C. M. Volk[2], M. R. Schoeberl[3], C. D. Boone[4], and P. F. Bernath[5,6]

[1]Department of Physics, University of York, Heslington, YO10 5DD, UK
[2]Department of Physics, University of Wuppertal, 42119 Wuppertal, Germany
[3]Science and Technology Corporation, Lanham, Maryland, 20706, USA
[4]Department of Chemistry, University of Waterloo, Ontario, Canada
[5]Department of Chemistry and Biochemistry, Old Dominion University, Virginia, USA
[6]Department of Chemistry, University of York, Heslington, YO10 5DD, UK

Correspondence to: A. T. Brown (alex.brown@york.ac.uk)

Abstract. Long lived halogen-containing compounds are important atmospheric constituents since they can act both as a source of chlorine radicals, which go on to catalyse ozone loss, and as powerful greenhouse gases. The long-term impact of these species on the ozone layer is dependent on their stratospheric lifetimes. Using observations from the Atmospheric Chemistry Experiment Fourier Transform Spectrometer (ACE-FTS) we present calculations of the stratospheric lifetimes of CFC-12, CCl$_4$, CH$_4$, CH$_3$Cl and N$_2$O. The lifetimes were calculated using the slope of the tracer–tracer correlation of these species with CFC-11 at the tropopause. The correlation slopes were corrected for the changing atmospheric concentrations of each species based on age of air and CFC-11 measurements from samples taken aboard the *Geophysica* aircraft – along with the effective linear trend of the volume mixing ratio (VMR) from tropical ground based AGAGE (Advanced Global Atmospheric Gases Experiment) sites. Stratospheric lifetimes were calculated using a CFC-11 lifetime of 45 yr. These calculations produced values of 113 + (−) 26 (18) yr (CFC-12), 35 + (−) 11 (7) yr (CCl$_4$), 69 + (−) 65 (23) yr (CH$_3$Cl), 123 + (−) 53 (28) yr (N$_2$O) and 195 + (−) 75 (42) yr (CH$_4$). The errors on these values are the weighted 1σ non-systematic errors. Systematic errors were estimated by recalculating lifetimes using VMRs which had been modified to reflect differences between ACE-FTS retrieved VMRs and those from other instruments. The re-

sults of these calculations, including systematic errors, were as follows: 113 + (−) 32 (20) for CFC-12, 123 + (−) 83 (35) for N$_2$O, 195 + (−) 139 (57) for CH$_4$, 35 + (−) 14 (8) for CCl$_4$ and 69 + (−) 2119 (34) yr for CH$_3$Cl. For CH$_3$Cl & CH$_4$ this represents the first calculation of the stratospheric lifetime using data from a space based instrument.

1 Introduction

Catalytic stratospheric ozone destruction occurs through the formation of halogen, nitrogen and hydrogen radicals. The halogen and nitrogen source gases also play a role in global radiative transfer blocking outgoing infrared radiation. In the case of halogen source gases, the long tropospheric lifetimes of many halogen-containing species allow them to reach the stratosphere through the upwelling tropical circulation. Once in the stratosphere they undergo photolysis and the halogen atoms which they contain are released into the surrounding atmosphere. Chlorine and bromine atoms released into the stratosphere catalyse ozone destruction. Fluorine atoms react rapidly to form stable HF. Chlorine-containing molecules typically absorb infrared radiation in the 650–780 cm^{-1} region (Lide, 1990; http://nwir.pnl.gov/), which is partly masked by CO$_2$ and water vapour absorption. Despite this, species such as CCl$_4$ have large global warming

potentials, for example CCl$_4$ has a global warming potential 1400 times larger than CO$_2$ (Solomon et al., 2007). C–F bonds typically absorb radiation in the 1400–1000 cm^{-1} region (http://nwir.pnl.gov/; Lide, 1990), a region which is relatively clear from atmospheric absorption from other species making fluorine-containing molecules powerful greenhouse gases. The emissions of many halogen-containing species are now limited under the Montreal Protocol (UNEP, 2009). The Montreal Protocol has been successful in both reducing the emissions of these species (Brown et al., 2011) and slowing the rate of ozone loss (Mäder et al., 2010). The reduction in the emission of ozone depleting substances has also had an effect in reducing the concentration of greenhouse gases (Velders et al., 2007).

A full analysis of ozone destruction must also take species such as N$_2$O, which is the major source of stratospheric NO and NO$_2$, and CH$_4$, which acts as a sink for atmospheric OH, into account. The long-term impact of these species on the environment is determined by their atmospheric lifetimes. Accurate estimates of atmospheric lifetimes of species which are directly and indirectly involved in stratospheric ozone loss are therefore vital. In particular, atmospheric lifetimes are used to set environmental policies on the emissions of ozone depleting substances and greenhouse gases. N$_2$O and methane are also greenhouse gases; furthermore, methane contributes to stratospheric water vapour, which can affect surface temperatures (Solomon et al., 2010).

The 2010 scientific assessment of ozone depletion report from the World Meteorology Organization (WMO) (Montzka et al., 2011) highlighted problems with the current lifetimes of some halogen-containing species such as carbon tetrachloride (CCl$_4$). Atmospheric concentrations of CCl$_4$ are declining more slowly than expected, which could be caused by an unreliable atmospheric lifetime (Montzka et al., 2011). This has led to the formation of the Stratospheric-Troposphere Processes And their Role in Climate (SPARC) lifetimes reassessment project. The aim of the re-evaluation is to estimate the numerical values of the lifetimes and the associated errors, assess the influence of different lifetime definitions and assess the effect of changing climate on lifetimes. The SPARC science report will be published by spring 2013 and will form the basis for the 2014 WMO Ozone Assessment (http://www.sparc-climate.org/activities/lifetime-halogen-gases/).

There are a number of methods for calculating the stratospheric lifetimes of long lived gases using satellite measurements. Stratospheric lifetimes can be calculated using a combination of satellite measurements and an atmospheric model. Satellite measurements are used to calculate the global atmospheric burden of a species. Subsequently, model data can be used to calculate the loss rates for the species from photolysis and chemical reaction. The instantaneous lifetime of a species is simply the global atmospheric burden divided by the sum of the loss rates (Johnston et al., 1979; Minschwaner et al., 1998). In situ measurements us-

ing balloon and aircraft borne instruments can be used to calculate stratospheric lifetimes of a number of long lived species using correlations with CFC-11 (Volk et al., 1997; Bujok et al., 2001; Laube et al., 2013). This method relies on accurate knowledge of the lifetime of CFC-11. Recent calculations of the lifetime of CFC-11, carried out using model data, have produced values between 56 and 64 yr (Douglass et al., 2008), whilst older estimates suggest a lifetime of 45 yr (Prinn et al., 1999). This uncertainty in the lifetime of CFC-11 therefore has a significant effect on the stratospheric lifetime estimates of a number of other halogen-containing species. If satellite data is to be used to carry out this analysis it should have sufficiently high vertical resolution to be able to extrapolate the slope of the correlation to the tropopause. Limb sounding satellite borne instruments, such as the Atmospheric Chemistry Experiment (ACE) and the Michelson Interferometer for Passive Atmospheric Sounding (MIPAS), have sufficiently high vertical resolution to be used for this method of lifetime calculation.

This paper presents new stratospheric lifetime estimates for CFC-12, CCl$_4$, CH$_4$, CH$_3$Cl and N$_2$O calculated from correlations with CFC-11 using data from Atmospheric Chemistry Experiment Fourier Transform Spectrometer (ACE-FTS). For CFC-12, CCl$_4$ and N$_2$O, which have no chemical sink in the troposphere, these lifetimes correspond to the global lifetime with respect to atmospheric removal.

2 Atmospheric Chemistry Experiment

Launched by NASA on board the Canadian satellite SCISAT-1 in August 2003, the ACE-FTS was designed to study "the chemical and dynamical processes that control the distribution of ozone in the stratosphere and upper troposphere" (Bernath, 2006). ACE-FTS was designed to build on the success of the Atmospheric Trace Molecule Spectroscopy (ATMOS) instrument. ATMOS flew on four separate shuttle flights, between 1985 and 1993, and pioneered space based observations of a number of halogenated gases (Irion et al., 2002; Gunson et al., 1996).

The ACE-FTS is a high resolution (0.02 cm^{-1}) spectrometer operating between 750 and 4400 cm^{-1}. ACE-FTS is a solar occultation instrument; a series of atmospheric absorption spectra are measured at a number of tangent heights during sunrise and sunset. Currently this method of measurement allows the retrieval of vertical profiles with high vertical resolution (1 km near the tropopause) of over 30 molecules (http://www.ace.uwaterloo.ca). The methodology used to retrieve the atmospheric volume mixing ratios (VMRs) of the different molecules from the ACE-FTS spectra is outlined by Boone et al. (2005). ACE-FTS has almost global coverage from the Antarctic to the Arctic due to the circular low Earth orbit with an inclination of 74° of SCISAT-1 (Bernath et al., 2005). The instrument has been in operation for ten years,

offering long-term observations of the volume mixing ratios of a number of atmospheric gases.

3 Method

The lifetime calculations presented in this paper follow the method laid out by Volk et al. (1997) based on the theoretical work of Plumb and Ko (1992) and Plumb (1996). In this section a brief outline of the method will be given; for a more complete discussion the reader is directed to the aforementioned paper.

The stratospheric lifetimes (τ_a, τ_b) of two long lived species, a and b, are related by the ratio of their average atmospheric VMR, $\bar{\sigma}$, and the slope of the correlation at the extratropical tropopause ($d\chi_a/d\chi_b$). In this paper we follow the convention of Volk et al. (1997), where χ refers to the (transient) mixing ratios and σ represents the mixing ratios corresponding to a steady state situation with the same tropopause mixing ratio.

$$\frac{\tau_a}{\tau_b} = \frac{\frac{\overline{\sigma_a}}{\overline{\sigma_b}}}{\frac{d\sigma_a}{d\sigma_b}\bigg|_{\text{tropopause}}} \tag{1}$$

This method can be used to calculate the relative lifetime of a long lived species, a, assuming that the lifetime of a second long lived species, b, is known. Conventionally lifetimes derived in this manner are calculated relative to CFC-11. Calculations are complicated by the fact that the observed VMRs (χ) of the species used in this study are changing independently of one another, while Eq. (1) requires steady-state quantities (σ). For the species considered here, the average VMRs for steady state ($\bar{\sigma}_i$) may well be approximated with the observed ones ($\bar{\chi}_i$) as the VMRs are nearly constant in the well-mixed troposphere that accommodates most of the species' burden. The transient correlation slopes at the tropopause, however, generally differ significantly from those in steady state. In order to account for the influence of tropospheric growth on the correlation slopes we use relations derived by Volk et al. (1997; Eqs. 25, 26, and A13 therein) between parameters relating to tropospheric growth, the width of the stratospheric age spectrum, and the gradients of a tracer's VMR with respect to stratospheric mean age (Γ) in steady state ($d\sigma/d\Gamma$) and non-steady state ($d\chi/d\Gamma$), at the tropopause:

$$\frac{d\sigma}{d\Gamma}\bigg|_{\Gamma=0} = \frac{\left(\frac{d\chi}{d\Gamma}\big|_{\Gamma=0} + \gamma_0\sigma_0\right)}{(1-2\gamma_0\Lambda)}, \tag{2}$$

$$\chi_0\left(t'\right) = \chi_0(t)\left[1 + b\left(t'-t\right) + c\left(t'-t\right)^2\right], \tag{3}$$

$$\gamma_0 = b - 2\Lambda c. \tag{4}$$

Volk et al. (1997) used a correction factor which was calculated using the correlation between the VMR of a species

and the age-of-air at the tropopause ($d\chi/d\Gamma$). The correction of $d\chi/d\Gamma$ to account for growth in the VMR of a species ($d\sigma/d\Gamma$ – Eq. 2) is complicated by a number of factors. The atmospheric growth rates of individual species are not necessarily linear. This necessitates the calculation of the effective linear growth rate (γ_0), and knowledge of the VMR of a species at the tropopause (σ_0). In order that γ_0 may be calculated, a long-term tropospheric data set for each species is required. A polynomial curve (Eq. 3) is fitted to this time series over a 5 yr interval prior to a specific reference time when the measurements were made (for example if the ACE-FTS measurement was made in 2009, $t = 2009$, $t' = $ year in which the individual ground based measurement in the time series was made). The fit coefficients, b and c (Eq. 3), can be used to calculate the γ_0 from Eq. (4). The second factor which complicates the process comes from the stratospheric age-of-air spectrum. The Λ factor in Eqs. (2) and (4) is the ratio of the squared width of the age spectrum to the mean age and accounts for the effects of the finite width of the age-of-air spectrum (Volk et al., 1997). For this work we have chosen to use a value of 1.25 yr for Λ following the work of Volk et al. (1997) and Laube et al. (2013). Rather than evaluating Eq. (2) for each species as done in Volk et al. (1997) we here combine it for two tracers a and b and substitute $d\chi_a/d\Gamma$ with $d\chi_a/d\chi_b \cdot d\chi_b/d\Gamma$, so that only the gradient with respect to mean age of tracer species b is required. This results in the following relation between the steady-state tracer–tracer correlation slope ($d\sigma_a/d\sigma_b$) required in Eq. (1) and the observed transient slope ($d\chi_a/d\chi_b$):

$$\frac{d\sigma_a}{d\sigma_b}\bigg|_{\text{tropopause}} = \frac{\frac{d\chi_a}{d\chi_b}\big|_{\text{tropopause}} \cdot \frac{d\chi_b}{d\Gamma}\big|_{\Gamma=0} + \gamma_{0_a}\sigma_{0_a}}{\frac{d\chi_b}{d\Gamma}\big|_{\Gamma=0} + \gamma_{0_b}\sigma_{0_b}}$$

$$\cdot \frac{1 - 2\gamma_{0_b}\Lambda}{1 - 2\gamma_{0_a}\Lambda} \tag{5}$$

The slope of the correlation of mean age against CFC-11 at the tropopause required in Eq. (5) was calculated by Laube et al. (2013) based on laboratory analysis of CFC-11 and SF$_6$ in whole air samples taken on board the *Geophysica* aircraft in October 2009 and January 2010. These calculations produced a value of -20.6 ± 4.6 ppt yr^{-1} for early 2010 for the slope at the tropopause. For other years this value has been scaled using the effective linear growth rate (γ_0) of CFC-11 during this time (the values for which can be seen in Table 2). The resulting values for the age-of-air slopes can be seen in Table 1. The use of the Laube et al. (2013) CFC-11 versus age-of-air slopes facilitates the comparisons of lifetimes calculated from ACE with those derived from the *Geophysica* samples by Laube et al. (2013). Initially we tested whether a correlation between model age data and ACE CFC-11 could contain the slopes but it was found that this was not the case.

Table 1. The slope of the age of air against the volume mixing ratio of CFC-11 at the tropopause.

	Age of air ppt yr^{-1}
2005	-21.3 ± 4.6
2006	-21.1 ± 4.6
2007	-20.9 ± 4.6
2008	-20.7 ± 4.6
2009	-20.6 ± 4.6
2010	-20.5 ± 4.6

4   Results and discussion

ACE-FTS data were divided into 24 separate data bins dependent on their stratospheric season and year. The data was first divided into 4 bins which corresponded with Northern Hemisphere stratospheric winter (NHW), Northern Hemisphere stratospheric summer (NHS), Southern Hemisphere stratospheric winter (SHW) and Southern Hemisphere stratospheric summer (SHS). These four bins were defined by the month in which the occultations were made in the following manner.

Northern Hemisphere Stratospheric Winter	November – December – January – February – March – April
Northern Hemisphere Stratospheric Summer	May* – June – July – August – September – October*
Southern Hemisphere Stratospheric Winter	May – June – July – August – September – October
Southern Hemisphere Stratospheric Summer	November* – December – January – February – March – April*

The months marked with asterisks are not truly stratospheric summer months; they were selected to increase the sample size used in this study. The NHW bin for 2005 would include data from November and December 2004 and from January, February, March and April 2005. Likewise, SHS 2005 included November and December 2004 and January, February, March and April 2005. The decision to use 6 month periods of analysis was made to increase the sample size used in this work. If seasonality has a significant effect on the calculated lifetime, dividing the data into two periods would be sufficient to see this difference.

Table 2. The effective linear growth rates (γ_0) in % yr^{-1} of CFC-11, CFC-12, CCl$_4$, CH$_4$, CH$_3$Cl and N$_2$O.

	CFC-11	CFC-12	CH$_3$Cl
2005	-0.853 ± 0.019	-0.181 ± 0.01	1.661 ± 0.556
2006	-0.92 ± 0.022	-0.286 ± 0.012	-0.428 ± 0.712
2007	-0.905 ± 0.023	-0.383 ± 0.011	0.665 ± 0.469
2008	-0.831 ± 0.026	-0.452 ± 0.013	0.862 ± 0.326
2009	-0.727 ± 0.019	-0.486 ± 0.012	-0.144 ± 0.291
2010	-0.718 ± 0.018	-0.478 ± 0.009	-0.384 ± 0.245

	CCl$_4$	N$_2$O	CH$_4$
2005	-0.933 ± 0.024	0.205 ± 0.007	0.003 ± 0.043
2006	-0.944 ± 0.026	0.212 ± 0.008	-0.034 ± 0.039
2007	-1.133 ± 0.032	0.217 ± 0.011	0.17 ± 0.059
2008	-1.305 ± 0.028	0.262 ± 0.008	0.477 ± 0.045
2009	-1.451 ± 0.023	0.257 ± 0.009	0.444 ± 0.046
2010	-1.479 ± 0.027	0.262 ± 0.009	0.328 ± 0.047

In the tropics, there is large-scale upwelling through the tropopause and further up in relative isolation from midlatitudes, resulting in tropical correlation curves different from those in the extratropical surf zone (e.g. Volk et al., 1996). Tropical correlations thus reflect local rather than global sources and sinks and are therefore not suited to derive global stratospheric lifetimes (Plumb, 1996; Neu and Plumb, 1999). In the higher latitudes, the polar vortex causes stratospheric air to subside in isolation from midlatitudes and correlation curves within the vortex develop separately from those at midlatitudes over the course of the winter (e.g. Plumb, 2007), thus making occultations within the polar vortex unsuitable for the derivation of stratospheric lifetimes. Tropical and polar latitudes thus act as lower and upper limits for the latitudes from which data can be used in this study. The latitudes used in this study run from above the tropics, 30° N/S to 70° N/S. Measurements made within the polar vortex appeared as outliers to the overall data and were removed as they fell outside of the median absolute deviation (MAD) filter. In this way both the tropical and the polar-regions are avoided. The division of the data into Northern and Southern hemispheres was designed to test whether there is any hemispheric dependence in the calculated lifetimes. By dividing the data seasonally the sensitivity of the calculated lifetimes to seasonal variation was also to be explored. Since the background VMR of these species varies annually the data was divided into additional bins inside of the four mentioned previously. These bins were separated by the year in which the occultations were made.

Once the data had been divided into the relevant bin, the data within the bins was filtered. Outlying data were removed from the ACE-FTS VMR profiles by excluding data whose deviation from the median was greater than 2.5 times the median absolute deviation (MAD) at each altitude. A MAD filter is an effective way to remove outlying data since the MAD is less susceptible to outliers than the standard

deviation. As has been mentioned previously, data within the polar vortex was outside these parameters and was therefore discarded during this stage of filtering. A final round of filtering removed data below the tropopause using tropopause altitudes from the ACE derived meteorological product (DMPs). Each ACE occultation has a unique DMP which presents the altitude of the tropopause at the latitude, longitude and local time of the occultation.

4.1 CFC-11 correlations

Mean correlation curves were produced for the correlations of each species vs. CFC-11. The mean correlation curves were calculated using the mean of the data in non-overlapping windows which were 2 ppt of CFC-11 wide. The error on the mean of this data in both x and y (where x is CFC-11 and y is the correlating species) is the standard error of the mean. These windows ran the entire range of the CFC-11 data beginning at the minimum concentration and moving along every 2 ppt until the maximum concentration value had been passed. Once a mean correlation curve had been produced the slope of the data within a moving window of 80 ppt of CFC-11 was calculated using a linear least squared fit which took both the error in the CFC-11 and the correlating species' mean into account. After measuring the slope of the data the window would be moved forwards by 5 ppt and the slope of the data would be calculated again. The procedure started 80 ppt of CFC-11 below the minimum CFC-11 VMR, providing a blank first reading. This procedure continued until the window was 80 ppt larger than the maximum CFC-11 VMR. At both ends of the data the windows contain areas with no data in them. In this case the middle of the data range was not the centre of the window. Instead, the centre of the window was amended to reflect the centre of the data. The same effect occurs at the tropopause. This produces a series of windows which become smaller and smaller the closer they get to the tropopause and the lower limit of the data. Once this procedure had been carried out data from windows corresponding to a CFC-11 VMR of less than 120 ppt were discarded and a second degree polynomial was fit to the remaining data. The data was weighted using the square of the inverse fitting errors on each point from the previous step. The aim of these calculations was to extrapolate the slope of the correlation to the tropopause. Removing data below 120 ppt of CFC-11 ensured that the polynomial fit would not be biased towards the higher altitudes. On the other hand, the range of the fit (120 to $\sim$220 ppt) ensured that the extrapolated slope at the tropopause would not be unduly affected from points directly at the tropopause where complex mixing from the troposphere can cause the observed correlation to breakdown. Examples of the correlation plots and slope calculations can be seen in Fig. 1, the remaining plots can be found in Appendix B (Figs. B1 to B21).

Fluxes of chemical species into the stratosphere from the tropopause are not constant and are prone to change as long as the species are not in steady state. This produces a curving effect in the correlations around the tropopause that can be clearly seen in Fig. 1. The method employed in this paper requires the knowledge of the slope of the stratospheric tracer–tracer correlation at the tropopause. The slope of the correlation at the tropopause was calculated using the equation derived from the polynomial fit along with the mean CFC-11 VMR at the tropopause. Following the work of Volk et al. (1979) statistical errors on the fit were calculated using a bootstrap method (Efron et al., 1991) and scaled using the number of independent points used in the extrapolation fit. The uncertainties in this work will first be evaluated and propagated on a purely statistical base. Potential systematic errors, which may be introduced during the retrieval process, will be discussed and taken into account at a later stage (cf. Sect. 4.2).

The slopes at the tropopause are shown in Table A1 in the section A of the appendix along with a plot of these slopes for comparison (Fig. A1). There are 3 bins with no correlation data, NHW 2005, SHW 2005 and NHW 2009. In these bins problems with the retrieval program, used to retrieve VMR from ACE-FTS spectra, caused a failure in the retrieval of CFC-11. Work is ongoing at this time to rectify this problem. Correlations between CFC-12 and CFC-11 produce slopes that range between 0.61 ± 0.04 and 1.25 ± 0.1. With a median (of all 24 bins) of 0.99 and a standard deviation of 0.19 these data exhibit good self consistency. The slopes of the CH$_3$Cl correlation show a significant spread with a maximum of 3.16 ± 2.25 and a minimum of 0.68 ± 0.39. The slopes have a median of 1.60 and a standard deviation of 0.65. CCl$_4$ has a large spread of slopes with a median of 0.59 and a standard deviation of 0.23. The maxima and minima of this data are 1.24 ± 0.26 and 0.18 ± 0.11. Both CH$_4$ and N$_2$O show relatively wide spreads of values with medians of 2026 and 577 and standard deviations of 914 and 178 respectively. One source of variation for CH$_3$Cl and CH$_4$ could be the flux of species across the tropopause, e.g. due to seasonal or interannual variations in tropospheric growth, leading to changes to the correlation slopes in the lowest part of the stratosphere.

The effective linear growth rate (γ_0 – Eq. 5) was calculated using monthly global means from the Advanced Global Atmospheric Gases Experiment (AGAGE) network (Prinn et al., 2000, 2001) for CFC-11 (Cunnold et al., 2002), CFC-12 (Cunnold et al., 1997), CCl$_4$ (Simmonds et al., 1998), CH$_4$ (Cunnold et al., 2002; Rigby et al., 2008), CH$_3$Cl (Simmonds et al., 2004; Cox et al., 2003) and N$_2$O (Prinn et al., 1990), following the method laid out in Volk et al. (1997) using Eqs. (3) and (4). For this study a quadratic function was fitted to 5 yr of AGAGE data prior to each year between 2005 and 2010. For CH$_3$Cl AGAGE data from between 2004 and 2010 was used. Strong seasonality was removed from the data using a sinusoidal term.

The VMRs at the tropopause (σ_0) were calculated by removing any data below 3 km below the tropopause and any data which lay above the tropopause. The remaining data was
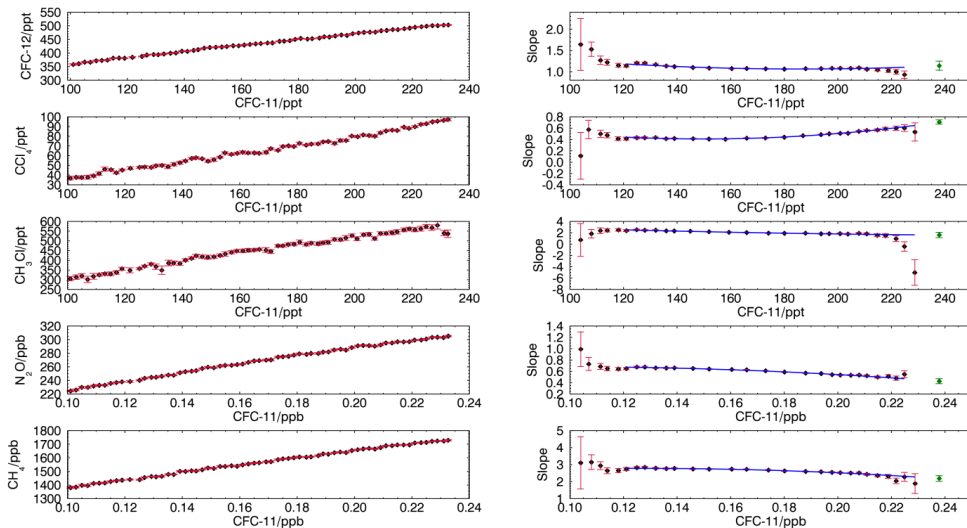
Fig. 1. Correlations between the volume mixing ratios of CFC-12, CCl$_4$, CH$_4$, CH$_3$Cl and N$_2$O and CFC-11 for the data from the Northern Hemisphere during the stratospheric winter of 2008. Left panels: the mean correlation curves. Each point represents the mean of the VMR, of both CFC-11 and CFC-12, in a window of 2 ppt of CFC-11. The error on these points is the standard deviation of the data within each 2 ppt window. Right panels: the local slope of data in an 80 ppt of CFC-11 window. The error on the points is the fitting error of this fit. The blue line is a second degree polynomial fit to the local slopes. The green point is the extrapolated slope at the tropopause.

used to calculate an annual mean VMR which represented σ_0; these values can be seen in Table A2 of Appendix A. The corrected correlation slopes, calculated using Eq. (5), can be found in Table A3 and Fig. A2 of Appendix A.

4.2 Lifetime calculations

The annual global mean atmospheric VMR ($\bar{\sigma}$) of each species was calculated using ACE-FTS profiles of the VMR (σ) weighted by atmospheric pressure (P). In this case pressure is being used as a proxy for density. Whilst using pressure will weight the lower stratosphere less than it deserves, giving a slight high bias in the atmospheric means, this effect will not be larger than the errors which are currently assigned to the means. Mean VMR profiles were calculated for each species in 15° latitude bins. Profiles were extended from their lowest point to the ground by assuming a constant VMR. Each VMR value was weighted by the corresponding pressure; this allowed a weighted mean to be calculated using equation 6. The global mean atmospheric VMRs were then calculated by weighting the pressure weighted means from the latitude bins using the cosine of the latitude. This was done since the majority of the mass of the global atmosphere is contained in the tropical troposphere. The results of this analysis can be seen in Table A4 of Appendix A.

$$\bar{\sigma} = \frac{\sum P_i \sigma_i}{\sum P_i} \qquad (6)$$

Calculations were carried out using a CFC-11 lifetime of 45 yr for ease of comparisons with previous studies. These lifetimes are presented in Table 3 (and as graphical represen-

tation in Fig. A3 in Appendix A). The final error on the calculated lifetimes results from propagation of the errors from each step of the calculation. As the overall error is dominated by the error of the measured correlation slope, which is (approximately) inverse proportional to the lifetime, the errors are asymmetric (but essentially symmetric for the inverse lifetime).

The calculated lifetimes show variations between the bins larger than the estimated statistical uncertainties (cf. Fig. A3). There are several factors that could contribute to such variability. First, the theoretical framework behind Eqs. (1) to (5) does not take seasonal or interannual variability into account, instead (1) relies on a steady-state situation, in which the correlation slope is related to the tracer flux into the stratosphere and thus (in steady state) to the stratospheric sink, while Eqs. (2–5) provide only a way to account for slow trends (i.e. variations on decadal scales). Seasonal to interannual variations of the flux into the stratosphere, on the other hand, can be expected to affect the correlation slopes and thus the derived lifetimes. Such flux variations can be caused by variability of transport to the stratosphere, but also by variability of tropospheric VMRs due to tropospheric transport and/or source variability. The latter would particularly concern species with natural sources and significant seasonal cycles (CH$_4$, N$_2$O, CH$_3$Cl), which indeed show the largest variation between the individual bins. Second, variability of transport within the stratosphere might affect the shape of the correlation curves and thus the extrapolated (and/or the real) correlation slope at the tropopause. Third, the variability of the lifetimes could be increased by interhemispheric

Table 3. The calculated lifetimes (yr) of CFC-12, CCl$_4$, CH$_4$, CH$_3$Cl and N$_2$O using a CFC-11 lifetime of 45 yr. NHS is Northern Hemisphere summer, NHW is Northern Hemisphere winter, SHS is Southern Hemisphere summer, SHW is Southern Hemisphere winter.

	Bin	CFC-12	CH$_3$Cl	CCl$_4$	N$_2$O	CH$_4$
2005	NHW	107 + (−)11(9)	123 + (−)156(43)	34 + (−)4(3)	−	−
	SHW	87 + (−)27(17)	34 + (−)170(16)	62 + (−)107(24)	91 + (−)12(10)	81 + (−)27(16)
2006	NHS	121 + (−)11(9)	−	49 + (−)20(11)	177 + (−)30(22)	218 + (−)42(31)
	NHW	89 + (−)15(12)	48 + (−)12(8)	24 + (−)3(2)	−	196 + (−)97(49)
	SHS	82 + (−)7(6)	35 + (−)7(5)	43 + (−)9(7)	153 + (−)44(28)	308 + (−)135(73)
	SHW	132 + (−)23(18)	123 + (−)149(44)	46 + (−)4(4)	85 + (−)10(8)	157 + (−)17(14)
2007	NHS	131 + (−)16(13)	−	23 + (−)2(2)	−	241 + (−)35(26)
	NHW	132 + (−)14(12)	−	41 + (−)8(6)	180 + (−)150(56)	221 + (−)72(44)
	SHS	90 + (−)14(11)	65 + (−)105(25)	46 + (−)27(13)	118 + (−)21(16)	231 + (−)50(35)
	SHW	95 + (−)8(7)	83 + (−)72(26)	35 + (−)3(3)	99 + (−)13(10)	136 + (−)19(15)
2008	NHS	96 + (−)6(6)	116 + (−)103(37)	30 + (−)2(2)	−	−
	NHW	87 + (−)9(8)	72 + (−)40(19)	28 + (−)2(2)	164 + (−)24(19)	202 + (−)32(22)
	SHS	121 + (−)15(12)	94 + (−)53(25)	32 + (−)4(3)	173 + (−)30(22)	−
	SHW	121 + (−)30(20)	83 + (−)91(29)	40 + (−)3(2)	113 + (−)16(12)	218 + (−)34(23)
2009	NHS	104 + (−)13(11)	−	17 + (−)4(3)	208 + (−)143(60)	204 + (−)57(36)
	NHW	−	−	−	−	−
	SHS	84 + (−)29(18)	−	28 + (−)8(5)	66 + (−)12(9)	89 + (−)41(21)
	SHW	109 + (−)7(7)	36 + (−)14(8)	36 + (−)9(6)	94 + (−)8(7)	222 + (−)30(21)
2010	NHS	150 + (−)11(10)	−	28 + (−)3(3)	185 + (−)54(34)	159 + (−)35(24)
	NHW	123 + (−)19(15)	49 + (−)29(13)	28 + (−)2(2)	95 + (−)17(13)	123 + (−)11(9)
	SHS	96 + (−)12(10)	70 + (−)108(27)	40 + (−)10(7)	120 + (−)23(17)	302 + (−)159(77)
	SHW	87 + (−)14(11)	54 + (−)51(18)	85 + (−)59(25)	100 + (−)11(9)	211 + (−)43(30)

differences due to the interhemispheric asymmetry in stratospheric transport. However, in situ measurements show no evidence for interhemispheric asymmetry or for drastic temporal variations of the correlation curves in the lower stratosphere, at least not on the seasonal scale (Volk et al., 1997). Finally, it is possible that the statistical errors estimated from each individual bin do not capture the full random error of the lifetime derivation. For example, the finite vertical resolution of the satellite data amounts to a certain amount of vertical smoothing of the trace gas profiles, which depends (through the shape of the profile) on the species and on time and latitude, and could potentially affect the correlation curves. Temporally and spatially inhomogeneous (i.e. non-random) sampling of the data within the bins could then lead to larger variability in the correlations between the bins than within a given bin. Most likely, all of the above factors combine to create the larger-than-expected variability in the derived lifetimes and it is not possible to separate and quantify these effects individually. However, we can analyse if the variability contains a significant seasonal signal and whether there are systematic hemispheric differences.

Weighted mean lifetimes were calculated for each seasonal and hemispheric combination and for all bins as average of the individual *inverse* lifetimes (quantities with nearly symmetric uncertainties as explained above), weighted using the inverse square of their largest error. As a measure for uncertainty, these weighted means were assigned the weighed standard deviation of the individual (inverse) lifetimes (again

a quantity symmetric for inverse lifetime, but asymmetric for lifetime). The various means and their uncertainties thus derived are shown in Table 4 for each species. It should be noted that in the case of the result for the Northern Hemisphere summer CH$_3$Cl calculated lifetime, due to problems caused within the fitting program it was only possible to produce one calculated lifetime for this bin. The mean lifetime reported here is therefore this calculated lifetime and associated error. As has been noted previously, the errors quoted here are the statistical uncertainties of the calculated results. Whilst the mean lifetimes calculated from the Northern Hemisphere (NH in Table 4) are longer than those calculated from the Southern Hemisphere (SH in Table 4) for CFC-12, CH$_3$Cl, and N$_2$O, they are shorter for CCl$_4$ and CH$_4$ and so it is hard to draw any solid conclusions from this fact. None of the variations between the hemispherically calculated lifetimes is larger than the combined errors on the lifetimes. Lifetimes calculated using summer data are smaller than those calculated using winter data for CFC-12, CH$_3$Cl, and CCl$_4$, but not for N$_2$O and CH$_4$. Variation between the seasonally calculated lifetimes is in fact always smaller than the error and this also holds for each hemisphere separately. Horizontal mixing in the stratosphere occurs due to breaking Rossby waves found during the winter in the extratropical surf zone (e.g. Plumb, 2002). The implication of this is that mixing occurs at a greater rate in the winter stratosphere than in the summer stratosphere. The mean lifetimes calculated here

Table 4. The mean lifetimes (yr) of CFC-12, CCl$_4$, CH$_4$, CH$_3$Cl and N$_2$O using a CFC-11 lifetime of 45 yr. NHS is Northern Hemisphere Summer, NHW is Northern Hemisphere Winter, SHS is Southern Hemisphere summer, SHW is Southern Hemisphere Winter, NH is Northern Hemisphere, SH is Southern Hemisphere.

	CFC-12	CH$_3$Cl	CCl$_4$	N$_2$O	CH$_4$
NHS	123 + (−)31(21)	116 + (−)102(37)	28 + (−)8(5)	182 + (−)12(10)	218 + (−)43(31)
NHW	111 + (−)25(17)	66 + (−)45(19)	30 + (−)5(4)	146 + (−)65(34)	161 + (−)69(37)
SHS	97 + (−)21(15)	58 + (−)68(20)	36 + (−)7(5)	136 + (−)68(34)	253 + (−)139(66)
SHW	106 + (−)15(12)	75 + (−)86(26)	42 + (−)8(6)	97 + (−)9(8)	189 + (−)62(37)
NH	119 + (−)29(19)	74 + (−)62(23)	29 + (−)6(4)	163 + (−)53(32)	188 + (−)76(42)
SH	103 + (−)18(13)	66 + (−)72(23)	41 + (−)9(6)	109 + (−)34(21)	200 + (−)78(44)
Summer	116 + (−)32(21)	69 + (−)103(26)	31 + (−)9(6)	153 + (−)69(36)	229 + (−)67(42)
Winter	108 + (−)19(14)	70 + (−)55(21)	36 + (−)11(7)	108 + (−)31(20)	179 + (−)65(38)
All data	113 + (−)26(18)	69 + (−)65(23)	35 + (−)11(7)	123 + (−)53(28)	195 + (−)75(42)

suggest that this phenomenon has not significantly affected our stratospheric lifetime calculations.

In summary, systematic hemispheric or seasonal differences are not apparent in the variations in lifetime between the individual bins, and within the given uncertainties (on the order of 20 % for CFC-12); our data are thus consistent with the universality of the tracer correlations found by Volk et al. (1997) over an interval of one year. Apparently significant variations in the lifetimes between individual bins (cf. Fig. A3) must then be explained by other factors as discussed above, i.e. variability of sources and/or atmospheric transport on interannual timescales and by errors not captured in the statistical uncertainty estimate for each individual bin. We assume here that the combination of these factors produces the apparently random variation in lifetimes displayed in Fig. A3. As our best estimate for the lifetimes, we thus use the weighted mean for all bins calculated as described above, and as a conservative estimate of uncertainty the weighted standard deviation of the individual bins. Note that, while the relative weights are derived from the estimated statistical errors for the individual bins (which vary due to differences in data quantity, making weighting a sensible choice), the overall statistical uncertainty is thus estimated from the variability between the bins. (Note also that the averaging and weighting is performed using the inverse of lifetime, for which the nearly symmetric individual errors, and thus weights, vary much less drastically than would appear in Fig. A3).

The calculated best estimates for lifetimes of CFC-12, CCl$_4$ and N$_2$O – 113 + (−) 26 (18), 35 + (−) 11 (7) and 123 + (−) 53 (28) yr, respectively – are within error of the lifetimes quoted by the WMO/IPCC: 100 (Montzka et al., 2011), 35 (Montzka et al., 2011) and 114 (Solomon et al., 2007) yr. The lifetime calculated for methane, of 195 + (−) 75 (42) yr, is significantly larger than that calculated by (Volk et al., 1997) of 93 ± 18 yr (also based on 45 yr for CFC-11). However, that latter value was derived from in situ data taken within one month and the quoted uncertainty may be an underestimate, as it does not account for the potential effect on the correlation slope of seasonal and interannual variations

of tropospheric CH$_4$. The stratospheric lifetime of CH$_3$Cl of 69 + (−) 65 (23) yr, reported here, represents the first calculations of the stratospheric lifetime of CH$_3$Cl and CH$_4$ using data from a space based instrument.

An analysis of the altitude dependent systematic errors in ACE-FTS retrievals has not been carried out at this time. However, ACE-FTS occultations have been compared to data from other instruments such as the MK-IV and FIRS-2 balloon borne spectrometers (e.g. Mahieu et al., 2008). Previous validation papers for N$_2$O, CH$_4$, CFC-11 and CFC-12 have not shown significant altitude dependent errors for the altitude range used in this study (Mahieu et al., 2008; Velazco et al., 2011). In addition to these comparisons, the profiles of CFC-11 and CFC-12 were compared to those from the SLIMCAT 3-D Chemical Transform Model (Brown et al., 2011). The profiles used in this work showed that, whilst there were differences in the VMR from ACE-FTS and from SLIMCAT the overall shapes of the profiles were extremely similar. The differences between VMRs from ACE-FTS and other instruments (mentioned previously) can be used as a proxy for the systematic error, due to the fact that the full systematic errors associated with ACE-FTS retrievals are not known at this time. The methods described in this section have been repeated using ACE-FTS VMRs which have been modified by the differences calculated in previous validation work. The values used to modify the VMRs were + 10 % for CFC-11 & CFC-12 from the validation work of Mahieu et al. (2008). Work by Velazco et al. (2011) also showed differences of +10 % for CH$_4$ and N$_2$O. The results of the reanalysis using these errors were combined with the statistical error. The final mean lifetimes were 113 + (−) 32 (20) for CFC-12, 123 + (−) 83 (35) for N$_2$O and 195 + (−) 139 (57) yr for CH$_4$.

The remaining species, CH$_3$Cl and CCl$_4$, are more problematic than the other species. Previous validations of these species have shown large differences between ACE-FTS retrievals and the retrievals from other species. For example comparisons between ACE-FTS and the MK-IV instrument (Velazco et al., 2011) found differences of 30 % in the VMR retrievals of CH$_3$Cl. The errors on ACE-FTS retrievals of

CCl$_4$ are estimated to be between 20 and 30 % (Allen et al., 2009). The estimation of systematic errors for the CCl$_4$ retrieval is complicated by the position of the spectral feature used to retrieve CCl$_4$ VMR. There is an interfering Q branch of CO$_2$, the line mixing of which is not properly accounted for in the forward model. Similarly, the Q branch of CH$_3$Cl suffers from line mixing which is not properly included in the forward model. The effects of line mixing on both of these retrievals are most serious in the troposphere, where the density of the atmosphere is at its greatest. In the stratosphere, where the density of the atmosphere is lower, line mixing becomes less of a problem within the retrieval. Quantifying the effects of line mixing on the retrieved VMR is a research project in and of itself. In this work we have approximated the systematic errors to be -30 % for CH$_3$Cl (Velazco et al., 2011) and $+20$ % for CCl$_4$ (Allen et al., 2009). Once more, lifetimes were calculated using VMR which had been modified by the corresponding systematic error. The final mean lifetimes for these species were $35 + (-) 14 (8)$ yr for CCl$_4$ and $69 + (-) 2119 (34)$ yr for CH$_3$Cl. These errors represent the best attempt to quantify the effect of systematic errors on the lifetimes of CCl$_4$ and CH$_3$Cl, however, due to the reasons outlined previously these errors may be different to those quoted here.

Recent model simulations have suggested CFC-11 lifetimes of between 56 and 64 yr (Douglass et al., 2008), differing from the older value of 45 yr which was used in the 2010 WMO report (Montzka et al., 2011). Changes to the lifetime of CFC-11 would naturally have an effect on the stratospheric lifetime of atmospheric species as calculated using correlations with CFC-11. For example using the range of CFC-11 lifetimes noted above produces a lifetime for CFC-12 which lies between 140 and 163 yr. The ratios of the lifetimes of CFC-12, CCl$_4$, CH$_4$, CH$_3$Cl and N$_2$O to CFC-11 are shown in Table 5 (with their statistical uncertainties). These values can be multiplied by the lifetime of CFC-11 to calculate the stratospheric lifetime of the species of interest. If the lifetime of CFC-11 is constrained further these ratios can be used to calculate new stratospheric lifetimes.

5 Conclusions

This paper presents calculations for the stratospheric lifetimes of CFC-12, CCl$_4$, CH$_4$, CH$_3$Cl and N$_2$O. The calculations were carried out using measurements made by the Atmospheric Chemistry Experiment Fourier Transform Spectrometer (ACE-FTS). The aim of this project was not only to calculate the stratospheric lifetimes of the species in question but also to test the assumptions which are intrinsic to these calculations. These assumptions are that there should be negligible hemispheric dependence in the calculated lifetimes and that there should be no seasonal dependence in the calculated lifetimes. To do this the data was divided into 24 bins representing stratospheric summer and winter in the

Table 5. The ratio of $\tau_\chi / \tau_{\mathrm{CFC\text{-}11}}$ for CFC-12, CCl$_4$, CH$_4$, CH$_3$Cl and N$_2$O.

Trace gas	Lifetime ratio to CFC-11
CFC-12	$2.5 + (-)0.57(0.39)$
CH$_3$Cl	$1.54 + (-)1.44(0.5)$
CCl$_4$	$0.77 + (-)0.25(0.15)$
N$_2$O	$2.74 + (-)1.18(0.63)$
CH$_4$	$4.33 + (-)1.66(0.94)$

Northern and Southern hemispheres for years between 2005 and 2010.

Stratospheric lifetimes were calculated using the slope of the correlation with CFC-11 at the tropopause which had to be corrected for changing atmospheric concentrations of each species. Stratospheric lifetimes were calculated using a lifetime of 45 yr for CFC-11. CFC-12 and N$_2$O are chemically inert in the troposphere and so their stratospheric lifetimes represent their atmospheric lifetimes. Calculated lifetimes showed no significant hemispheric or seasonal dependency. This suggested that for relative lifetime calculations the hemispheres are identical throughout the year at least within the given spread of values (on the order of 20 %, for CFC-12). Individual lifetimes calculated for CH$_3$Cl, N$_2$O and CH$_4$ displayed a large spread of values (about 48, 30 and 28 % respectively), presumably in part caused by variability of their tropospheric sources affecting the flux into the stratosphere.

Weighted means were calculated by weighting the individual (inverse) lifetimes by the reciprocal of the square of their error. These calculations produced values of $113 + (-) 26 (18)$ yr (CFC-12), $35 + (-) 11 (7)$ yr (CCl$_4$), $195 + (-) 75 (42)$ yr (CH$_4$), $69 + (-) 65 (23)$ yr (CH$_3$Cl) and $123 + (-) 53 (28)$ yr (N$_2$O). The calculated lifetimes of CFC-12, CCl$_4$ and N$_2$O are within error of the lifetimes quoted by the WMO/IPCC: 100 (Montzka et al., 2011), 35 (Montzka et al., 2011) and 114 (Solomon et al., 2007) yr. The lifetime calculated for methane, of $195 + (-) 75 (42)$ yr, is significantly larger than that calculated by Volk et al. (1997) of 93 ± 18 yr. The altitude dependent systematic errors in ACE-FTS retrievals are not currently known. An attempt has been made to estimate the effect of systematic errors on the calculated lifetimes. Lifetimes were recalculated using VMRs which had been modified to reflect differences between ACE-FTS retrieved VMRs and those from other instruments. The mean lifetimes were unaffected by these calculations, which affected the error ranges of these calculations. The results of these calculations were as follows: $113 + (-) 32 (20)$ for CFC-12, $123 + (-) 83 (35)$ for N$_2$O, $195 + (-) 139 (57)$ for CH$_4$, $35 + (-) 14 (8)$ for CCl$_4$ and $69 + (-) 2119 (34)$ yr for CH$_3$Cl. The lifetimes calculated in this work are relative to the lifetime of CFC-11 (45 yr), thus if the lifetime of CFC-11 changes so will the lifetime of these species.

Appendix A

Table A1. The slopes of the correlations of CFC-12, CCl$_4$, CH$_4$, CH$_3$Cl and N$_2$O with CFC-11, extrapolated to the tropopause. NHS is Northern Hemisphere summer, NHW is Northern Hemisphere winter, SHS is Southern Hemisphere summer, SHW is Southern Hemisphere winter. Data with errors greater than the correlations have been removed.

	Bin	CFC-12	CH$_3$Cl	CCl$_4$	N$_2$O	CH$_4$
2005	NHW	0.96 ± 0.08	1.21 ± 0.37	0.6 ± 0.07	–	–
	SHW	1.19 ± 0.29	3.16 ± 2.24	0.31 ± 0.22	716.81 ± 75.47	4403.1 ± 1080.64
2006	NHS	0.82 ± 0.06	–	0.41 ± 0.13	386.3 ± 47.25	1609.02 ± 257.51
	NHW	1.14 ± 0.17	1.91 ± 0.37	0.89 ± 0.1	–	1794.21 ± 599.76
	SHS	1.25 ± 0.1	2.68 ± 0.43	0.47 ± 0.09	441.96 ± 89.48	1130.28 ± 348.86
	SHW	0.75 ± 0.12	0.68 ± 0.39	0.44 ± 0.03	764.16 ± 66.93	2240.74 ± 193.1
2007	NHS	0.73 ± 0.08	–	0.91 ± 0.07	–	1631.25 ± 154.93
	NHW	0.72 ± 0.07	–	0.48 ± 0.08	384.17 ± 158.75	1768.92 ± 385.62
	SHS	1.1 ± 0.16	1.71 ± 0.93	0.42 ± 0.18	568.32 ± 76.45	1694.7 ± 255.45
	SHW	1.04 ± 0.08	1.38 ± 0.52	0.57 ± 0.05	668.52 ± 63.26	2775.14 ± 288.66
2008	NHS	1.02 ± 0.06	1.08 ± 0.38	0.67 ± 0.05	–	–
	NHW	1.14 ± 0.11	1.6 ± 0.47	0.71 ± 0.04	425.58 ± 43.92	2180.86 ± 171.34
	SHS	0.79 ± 0.09	1.29 ± 0.36	0.61 ± 0.06	405.89 ± 48.77	–
	SHW	0.78 ± 0.17	1.43 ± 0.61	0.48 ± 0.03	599.92 ± 61.47	2049.66 ± 145.78
2009	NHS	0.92 ± 0.11	–	1.24 ± 0.26	342.99 ± 122.16	2139.97 ± 351.11
	NHW	–	–	–	–	–
	SHS	1.17 ± 0.34	–	0.72 ± 0.18	992.12 ± 144.53	4408.87 ± 1253.71
	SHW	0.87 ± 0.05	2.72 ± 0.75	0.54 ± 0.12	710.83 ± 43.07	1997.24 ± 111.75
2010	NHS	0.61 ± 0.04	–	0.71 ± 0.08	386.97 ± 74.89	2566.37 ± 387.05
	NHW	0.76 ± 0.11	1.95 ± 0.76	0.72 ± 0.04	716.72 ± 98.31	3244.25 ± 157.55
	SHS	1.01 ± 0.12	1.34 ± 0.87	0.47 ± 0.11	572.71 ± 81.13	1485.76 ± 396.57
	SHW	1.14 ± 0.17	1.77 ± 0.92	0.18 ± 0.1	680.5 ± 55.37	2003.68 ± 256.47

Table A2. The mean volume mixing ratio at the tropopause (σ_0).
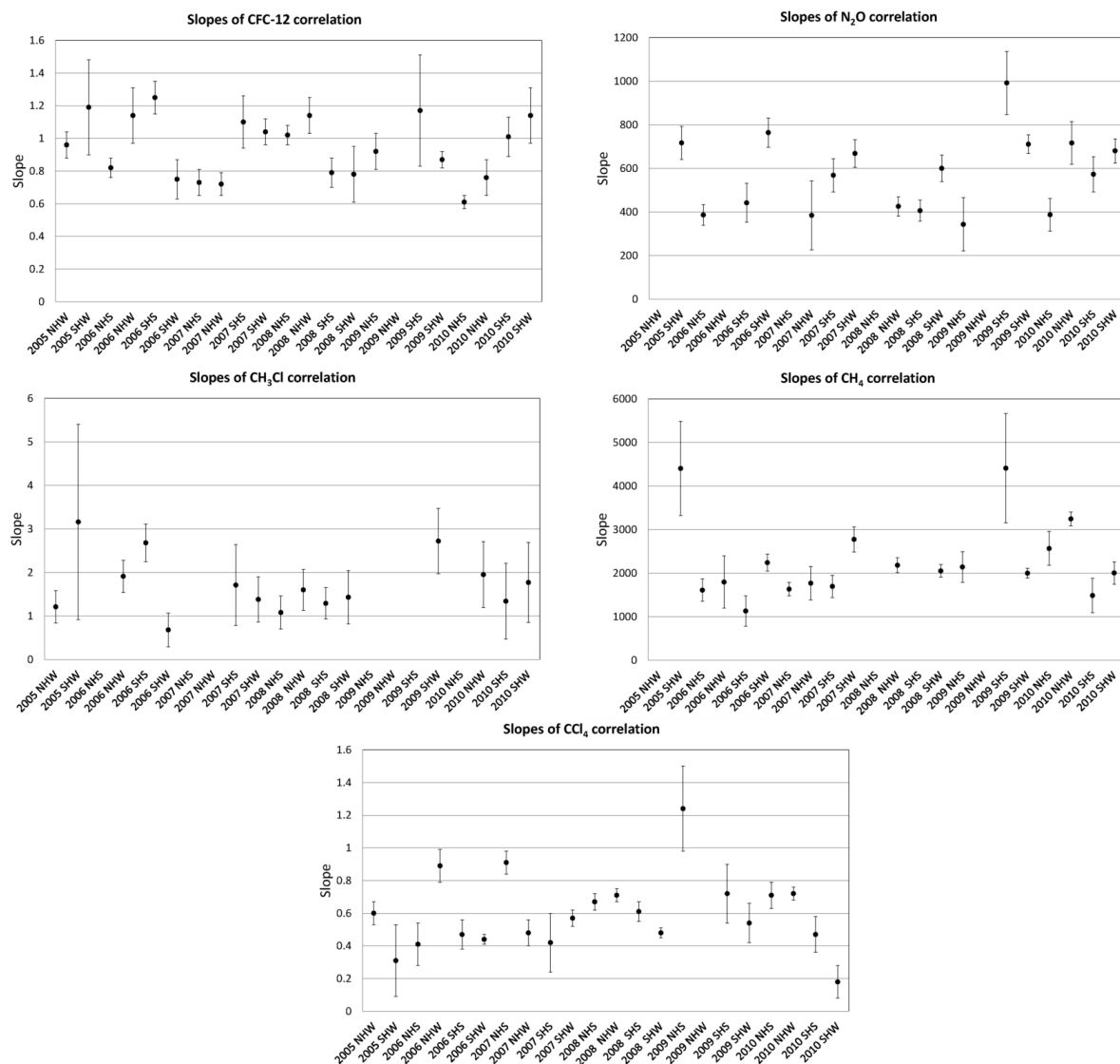
	CFC-11	CFC-12	CH$_3$Cl	CCl$_4$	N$_2$O	CH$_4$
2005	245.24 ± 3.14	515.63 ± 4.88	575.6 ± 9.86	106.33 ± 3.14	315.3 ± 2	1747.5 ± 33.4
2006	240.9 ± 3	512.54 ± 7.82	586.4 ± 27.78	106.83 ± 7.34	315.7 ± 2.5	1755.8 ± 36.2
2007	238.23 ± 1.72	510.97 ± 4.19	612.36 ± 25.76	106.59 ± 7.8	316.5 ± 0.7	1762.6 ± 34.9
2008	237.84 ± 3.03	509.52 ± 5.94	571.52 ± 39.13	104.51 ± 6.89	317.4 ± 2	1765.5 ± 36.1
2009	235.54 ± 4.54	510.17 ± 7.25	596.21 ± 11.75	105.45 ± 9.15	317.7 ± 2.2	1770 ± 26.2
2010	232 ± 2.72	503.36 ± 6.83	572.45 ± 23.35	101.29 ± 7.47	317.3 ± 4.4	1770.5 ± 38.2

Table A3. The corrected slopes of the correlations of CFC-12, CCl$_4$, CH$_4$, CH$_3$Cl and N$_2$O with CFC-11, extrapolated to the tropopause. NHS is Northern Hemisphere summer, NHW is Northern Hemisphere winter, SHS is Southern Hemisphere summer, SHW is Southern Hemisphere winter.

	Bin	CFC-12	CH$_3$Cl	CCl$_4$
2005	NHW	0.93 + (−)0.08(0.08)	0.74 + (−)0.4(0.41)	0.59 + (−)0.06(0.06)
	SHW	1.15 + (−)0.27(0.27)	2.63 + (−)2.18(2.19)	0.32 + (−)0.2(0.2)
2006	NHS	0.82 + (−)0.06(0.06)	–	0.41 + (−)0.12(0.12)
	NHW	1.11 + (−)0.16(0.16)	1.86 + (−)0.37(0.37)	0.85 + (−)0.09(0.09)
	SHS	1.21 + (−)0.09(0.09)	2.56 + (−)0.42(0.42)	0.47 + (−)0.08(0.08)
	SHW	0.75 + (−)0.11(0.11)	0.73 + (−)0.4(0.4)	0.44 + (−)0.03(0.03)
2007	NHS	0.76 + (−)0.08(0.08)	–	0.87 + (−)0.07(0.07)
	NHW	0.75 + (−)0.07(0.07)	–	0.48 + (−)0.08(0.08)
	SHS	1.1 + (−)0.14(0.14)	1.43 + (−)0.88(0.88)	0.43 + (−)0.16(0.16)
	SHW	1.04 + (−)0.08(0.08)	1.11 + (−)0.51(0.52)	0.57 + (−)0.05(0.05)
2008	NHS	1.04 + (−)0.05(0.05)	0.81 + (−)0.37(0.38)	0.67 + (−)0.04(0.04)
	NHW	1.15 + (−)0.1(0.1)	1.3 + (−)0.45(0.46)	0.7 + (−)0.03(0.03)
	SHS	0.83 + (−)0.09(0.09)	1 + (−)0.35(0.36)	0.61 + (−)0.06(0.06)
	SHW	0.82 + (−)0.16(0.16)	1.13 + (−)0.59(0.59)	0.49 + (−)0.02(0.02)
2009	NHS	0.97 + (−)0.1(0.1)	–	1.19 + (−)0.23(0.23)
	NHW	–	–	–
	SHS	1.2 + (−)0.31(0.31)	–	0.72 + (−)0.17(0.17)
	SHW	0.92 + (−)0.04(0.05)	2.58 + (−)0.71(0.71)	0.56 + (−)0.11(0.11)
2010	NHS	0.67 + (−)0.04(0.04)	–	0.71 + (−)0.07(0.07)
	NHW	0.82 + (−)0.11(0.11)	1.92 + (−)0.71(0.71)	0.72 + (−)0.04(0.04)
	SHS	1.05 + (−)0.11(0.11)	1.35 + (−)0.82(0.82)	0.5 + (−)0.1(0.1)
	SHW	1.17 + (−)0.16(0.16)	1.75 + (−)0.86(0.86)	0.23 + (−)0.1(0.1)

	Bin	N$_2$O	CH$_4$
2005	NHW	–	–
	SHW	641.7 + (−)72.5(74.6)	4093 + (−)1008.3(1011.1)
2006	NHS	330 + (−)45.5(47.2)	1514.5 + (−)241.2(242.5)
	NHW	–	1685.8 + (−)556.3(556.9)
	SHS	381.8 + (−)84.3(85.3)	1071.7 + (−)324.4(324.8)
	SHW	681.7 + (−)65.1(67.9)	2098.9 + (−)184.5(187.9)
2007	NHS	–	1385.4 + (−)159.1(168.1)
	NHW	327.5 + (−)148.5(149)	1513.6 + (−)365.6(369.9)
	SHS	499.2 + (−)72.9(74.6)	1444.5 + (−)247.3(253.5)
	SHW	592.6 + (−)61.4(63.9)	2450.4 + (−)281.3(291.2)
2008	NHS	–	–
	NHW	361.7 + (−)43.3(45.7)	1674.3 + (−)193.2(222.5)
	SHS	343.2 + (−)47.6(49.6)	–
	SHW	525.2 + (−)60(62.5)	1550.5 + (−)172.3(203.4)
2009	NHS	287 + (−)116.1(116.8)	1671.6 + (−)348.4(363.6)
	NHW	–	–
	SHS	901.2 + (−)138.5(140.3)	3828.4 + (−)1199.3(1207.5)
	SHW	635 + (−)44.2(47.9)	1535.9 + (−)144.3(176.8)
2010	NHS	328.1 + (−)72(73.3)	2166.2 + (−)378.5(389.8)
	NHW	640.6 + (−)94.8(96.6)	2809.5 + (−)180.4(208.2)
	SHS	504.1 + (−)78.3(80.1)	1140.6 + (−)384.2(391.7)
	SHW	606.3 + (−)55.1(58)	1632.1 + (−)257.4(270.9)

Table A4. Mean atmospheric volume mixing ratio ($\bar{\sigma}$).

	CFC-11	CFC-12	CH$_3$Cl	CCl$_4$	N$_2$O	CH$_4$
2005	230.31 ± 5.74	508.14 ± 13.75	463.23 ± 12.83	103.28 ± 2.67	299 ± 8.0	1689 ± 44.9
2006	230.27 ± 6.22	505.64 ± 13.67	458.31 ± 3.64	103.56 ± 2.87	298.1 ± 8.0	1689.6 ± 44.9
2007	227.95 ± 6.20	502.6 ± 13.63	468.97 ± 13.08	100.25 ± 2.77	297.9 ± 7.9	1690.7 ± 44.8
2008	225.61 ± 6.07	500.15 ± 13.51	470.97 ± 13.15	99.2 ± 2.72	296.9 ± 7.9	1695.8 ± 45.0
2009	222.6 ± 6.04	497.68 ± 13.48	456.11 ± 12.73	98.48 ± 2.73	295.5 ± 7.9	1683.4 ± 44.7
2010	221.03 ± 6.00	495.96 ± 13.39	462.15 ± 12.77	97.52 ± 2.67	298.1 ± 7.9	1694.4 ± 44.8

Fig. A1. A graphical representation of the slopes of the various correlations with CFC-11. The data is presented in the same order as it appears in Table A1.
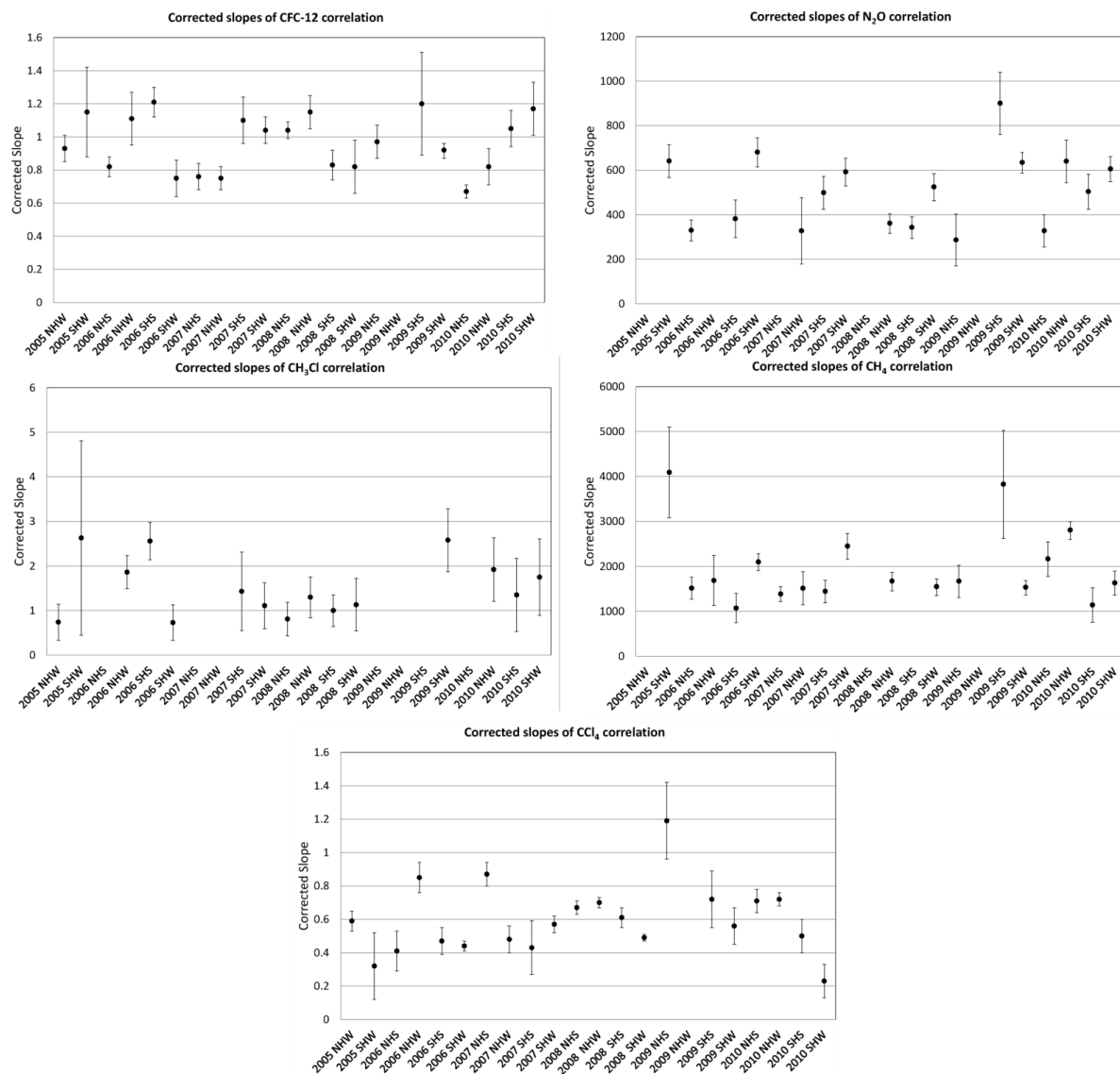
Fig. A2. A graphical representation of the corrected slopes of the various correlations with CFC-11. The data is presented in the same order as it appears in Table A3.
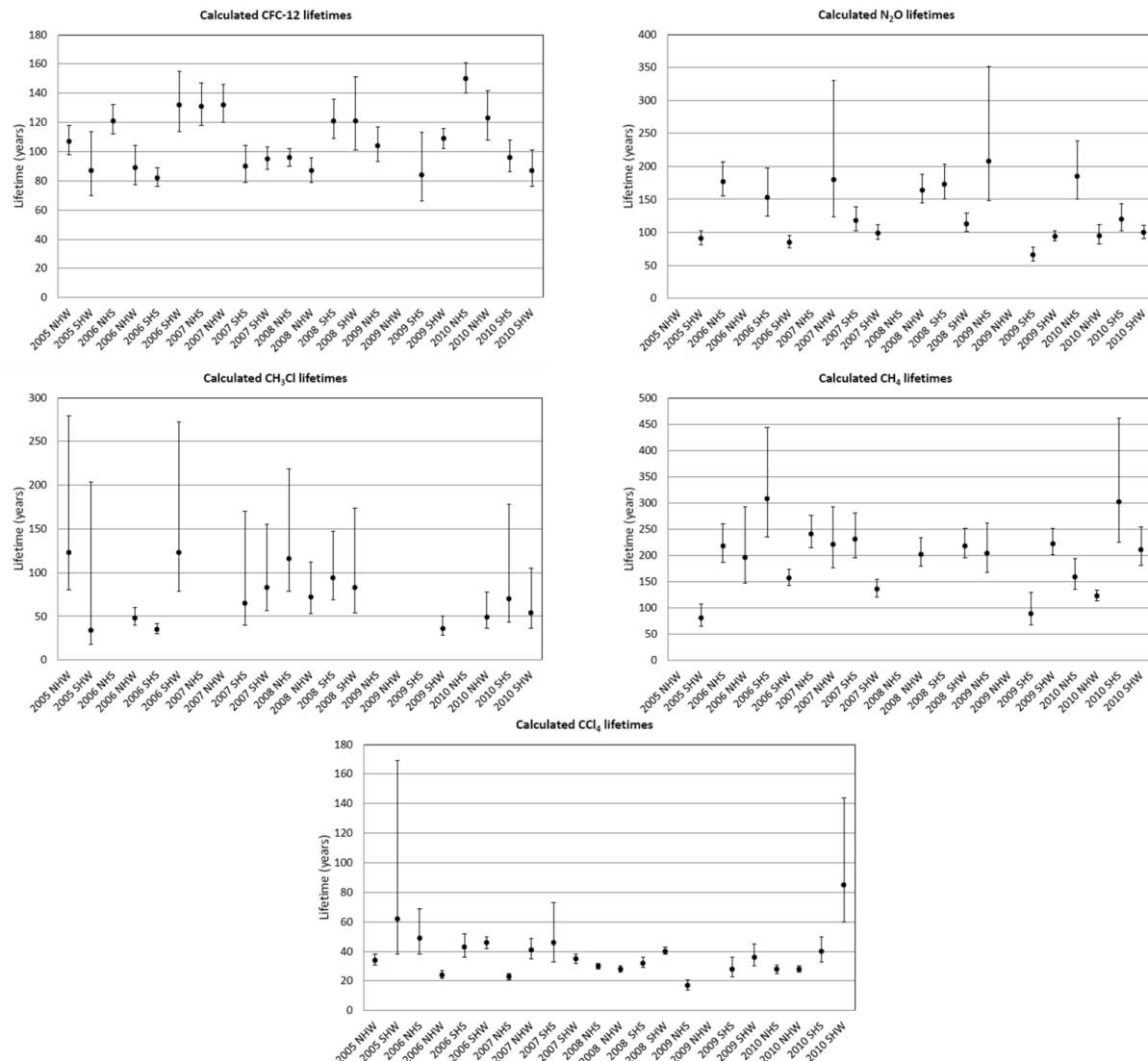
Fig. A3. A graphical representation of the lifetimes of CFC-12, CCl$_4$, CH$_3$Cl, N$_2$O and CH$_4$ calculated using a CFC-11 of 50 yr. The data is presented in the same order as it appears in the main paper.

Appendix B

Correlation plots: in this section the correlation plots used in this work are shown. Species where the fit to the data failed are not included in these plots
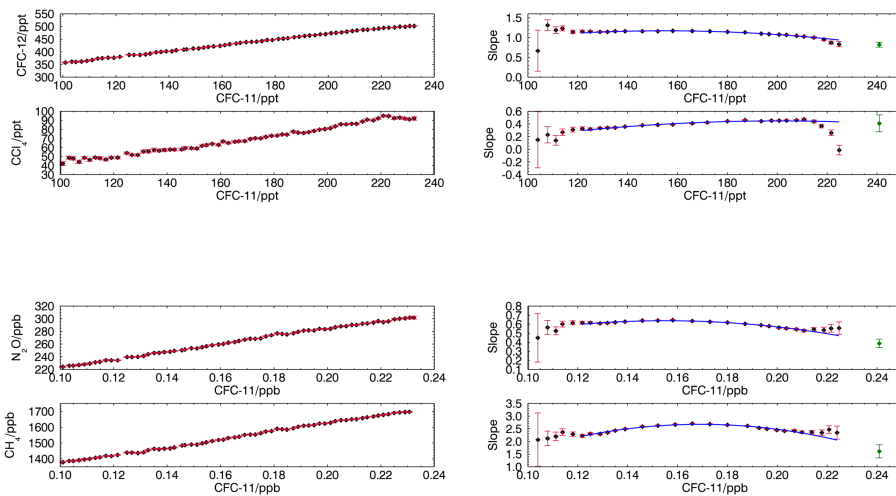
Fig. B1. Correlations between the volume mixing ratios of CFC-12, CCl$_4$, CH$_4$, and N$_2$O and CFC-11 for the data from the Northern Hemisphere during the stratospheric summer of 2006. Left panels: the mean correlation profile. Each point represents the mean of the VMR in a window of 2 ppt of CFC-11. The error on these points is the standard deviation of the data within each 2 ppt window. Right panels: the local slope of data in an 80 ppt of CFC-11 window. The error on the points is the fitting error of this fit. The blue line is a second degree polynomial fit to the local slopes. The green point is the extrapolated slope at the tropopause.
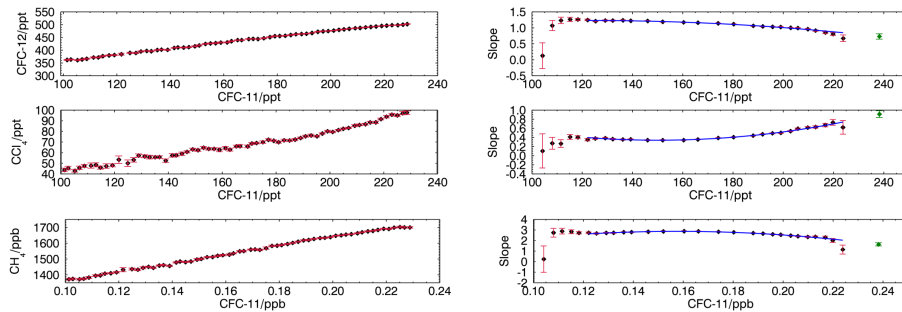
Fig. B2. Correlations between the volume mixing ratios of CFC-12, CCl$_4$, and CH$_4$ and CFC-11 for the data from the Northern Hemisphere during the stratospheric summer of 2007. Panel descriptions as in Fig. B1.
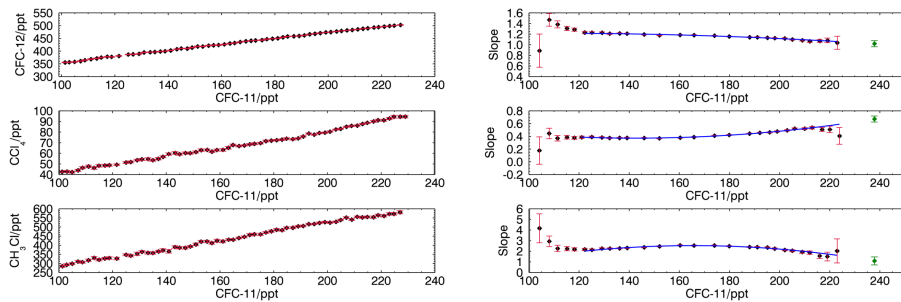
Fig. B3. Correlations between the volume mixing ratios of CFC-12, CCl$_4$, and CH$_3$Cl and CFC-11 for the data from the Northern Hemisphere during the stratospheric summer of 2008. Panel descriptions as in Fig. B1.
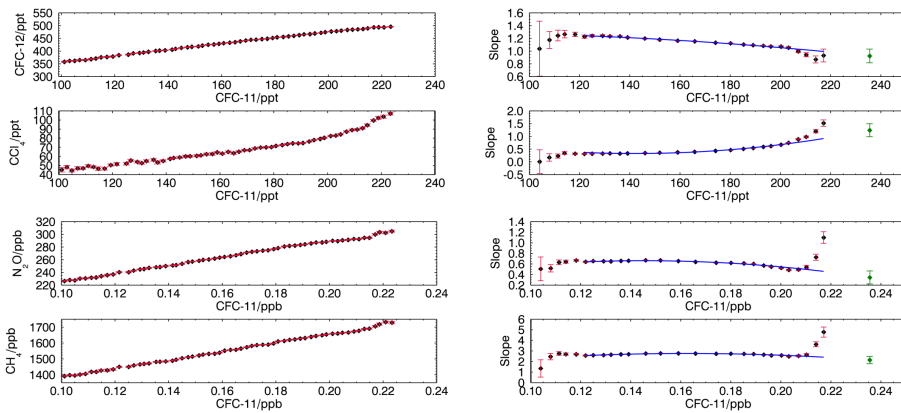
Fig. B4. Correlations between the volume mixing ratios of CFC-12, CCl$_4$, CH$_4$ and N$_2$O and CFC-11 for the data from the Northern Hemisphere during the stratospheric summer of 2009. Panel descriptions as in Fig. B1.
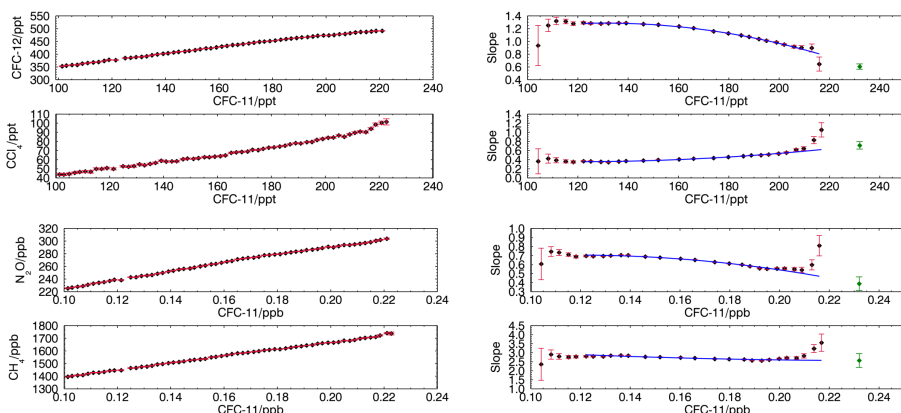
Fig. B5. Correlations between the volume mixing ratios of CFC-12, CCl$_4$, CH$_4$ and N$_2$O and CFC-11 for the data from the Northern Hemisphere during the stratospheric summer of 2010. Panel descriptions as in Fig. B1.
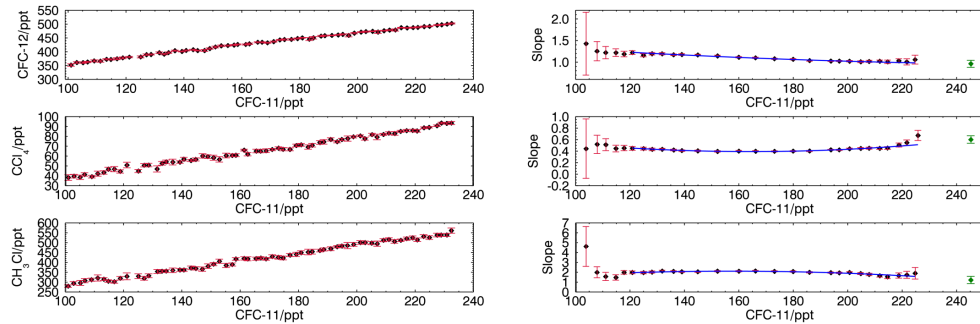
Fig. B6. Correlations between the volume mixing ratios of CFC-12, CCl$_4$ and CH$_3$Cl and CFC-11 for the data from the Northern Hemisphere during the stratospheric winter of 2005. Panel descriptions as in Fig. B1.
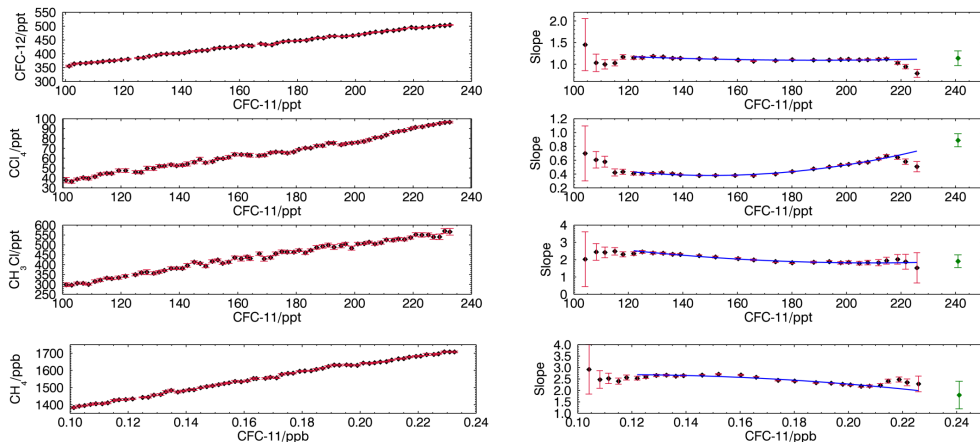
Fig. B7. Correlations between the volume mixing ratios of CFC-12, CCl$_4$, CH$_4$ and CH$_3$Cl and CFC-11 for the data from the Northern Hemisphere during the stratospheric winter of 2006. Panel descriptions as in Fig. B1.
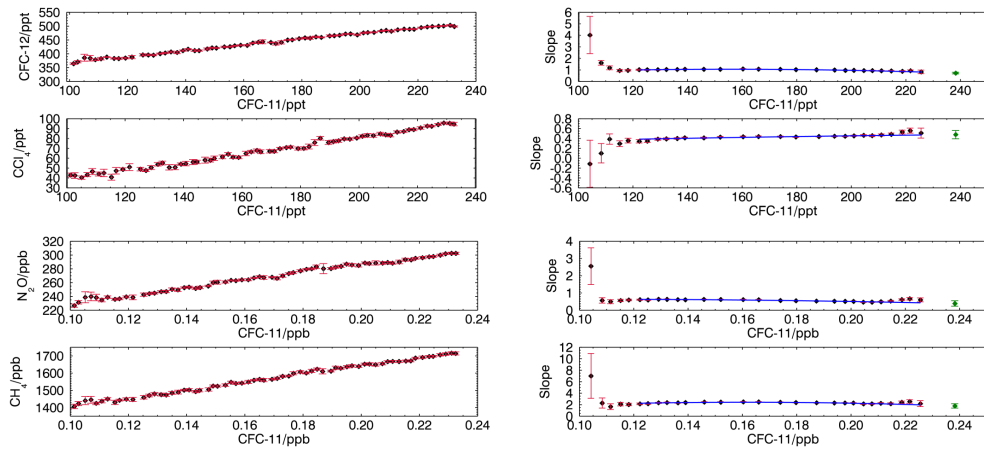
Fig. B8. Correlations between the volume mixing ratios of CFC-12, CCl$_4$, CH$_4$ and N$_2$O and CFC-11 for the data from the Northern Hemisphere during the stratospheric winter of 2007. Panel descriptions as in Fig. B1.
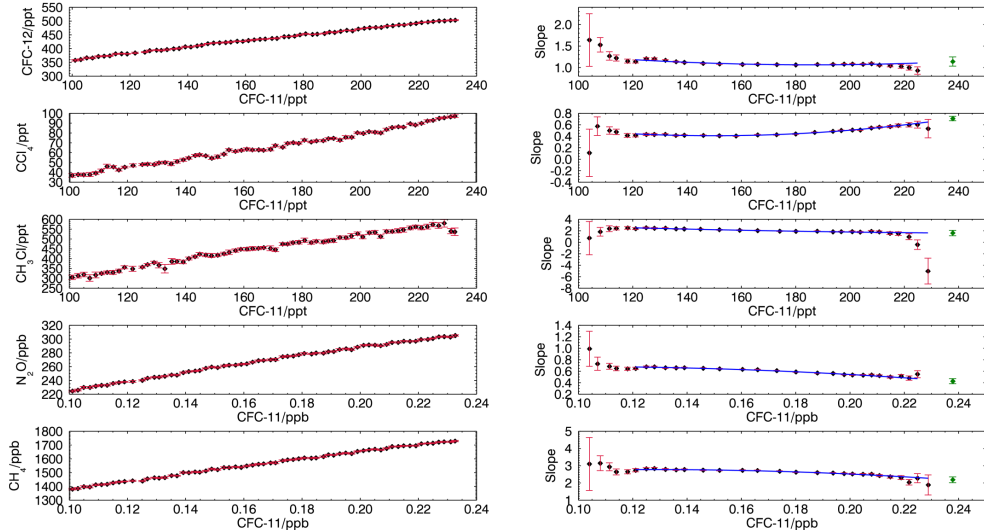
Fig. B9. Correlations between the volume mixing ratios of CFC-12, CCl$_4$, CH$_4$, CH$_3$Cl and N$_2$O and CFC-11 for the data from the Northern Hemisphere during the stratospheric winter of 2008. Panel descriptions as in Fig. B1.
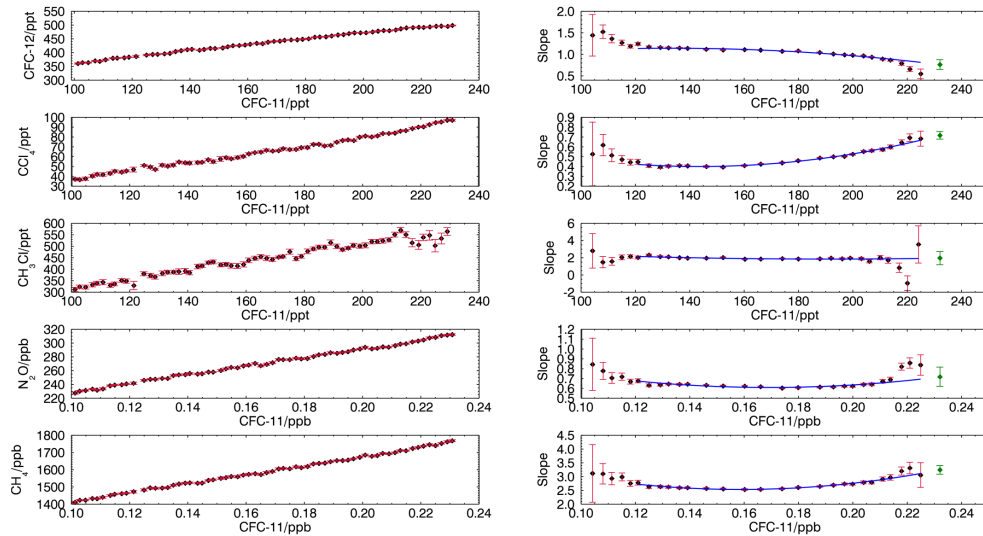
Fig. B10. Correlations between the volume mixing ratios of CFC-12, CCl$_4$, CH$_4$, CH$_3$Cl and N$_2$O and CFC-11 for the data from the Northern Hemisphere during the stratospheric winter of 2010. Panel descriptions as in Fig. B1.
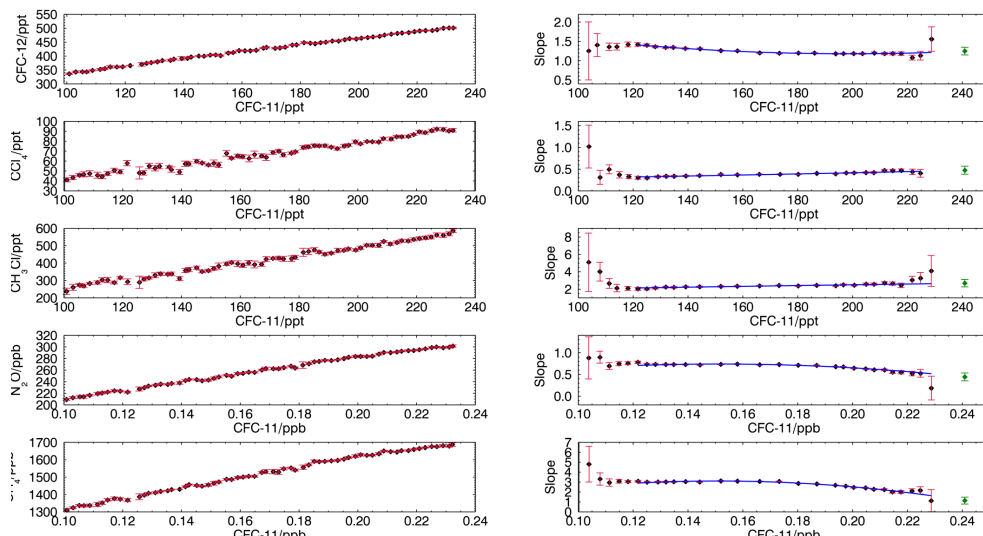
Fig. B11. Correlations between the volume mixing ratios of CFC-12, CCl$_4$, CH$_4$, CH$_3$Cl and N$_2$O and CFC-11 for the data from the Southern Hemisphere during the stratospheric summer of 2006. Panel descriptions as in Fig. B1.
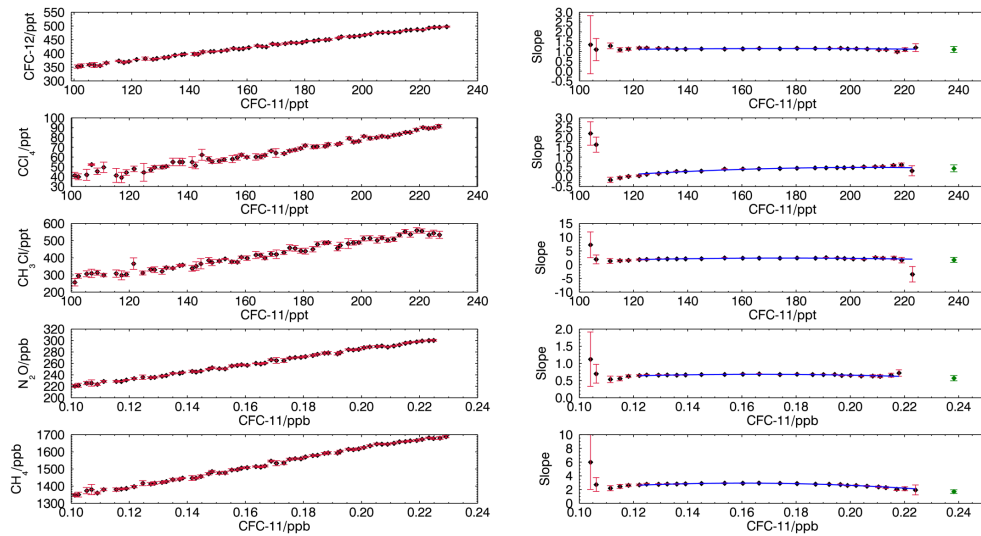
Fig. B12. Correlations between the volume mixing ratios of CFC-12, CCl$_4$, CH$_4$, CH$_3$Cl and N$_2$O and CFC-11 for the data from the Southern Hemisphere during the stratospheric summer of 2007. Panel descriptions as in Fig. B1.
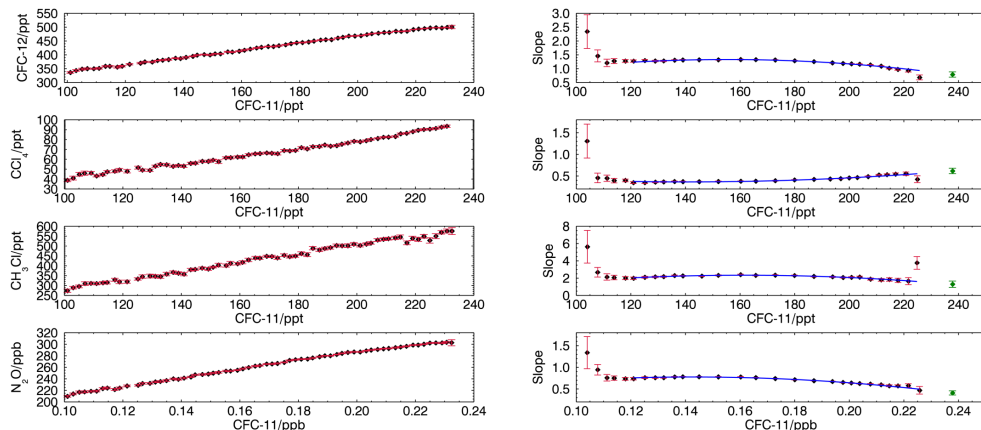
Fig. B13. Correlations between the volume mixing ratios of CFC-12, CCl$_4$, CH$_3$Cl and N$_2$O and CFC-11 for the data from the Southern Hemisphere during the stratospheric summer of 2008. Panel descriptions as in Fig. B1.
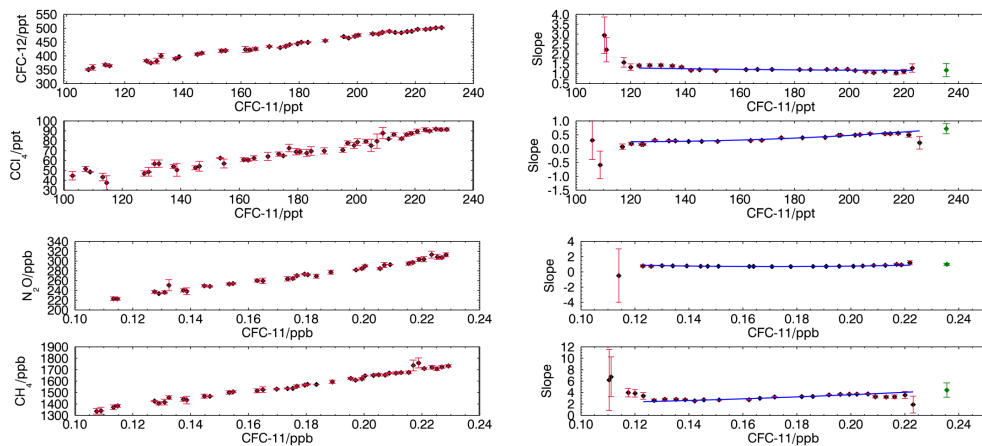
Fig. B14. Correlations between the volume mixing ratios of CFC-12, CCl$_4$, CH$_4$ and N$_2$O and CFC-11 for the data from the Southern Hemisphere during the stratospheric summer of 2009. Panel descriptions as in Fig. B1.
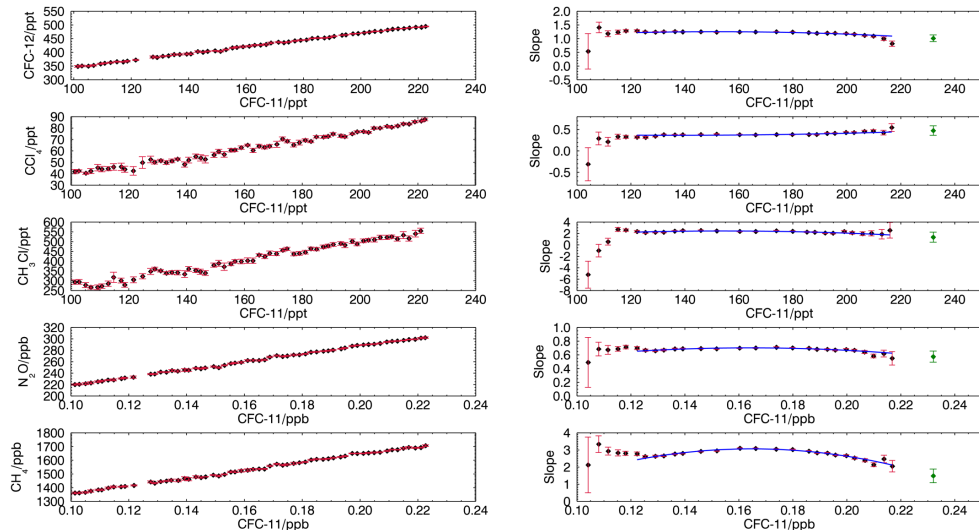
Fig. B15. Correlations between the volume mixing ratios of CFC-12, CCl$_4$, CH$_4$, CH$_3$Cl and N$_2$O and CFC-11 for the data from the Southern Hemisphere during the stratospheric summer of 2010. Panel descriptions as in Fig. B1.
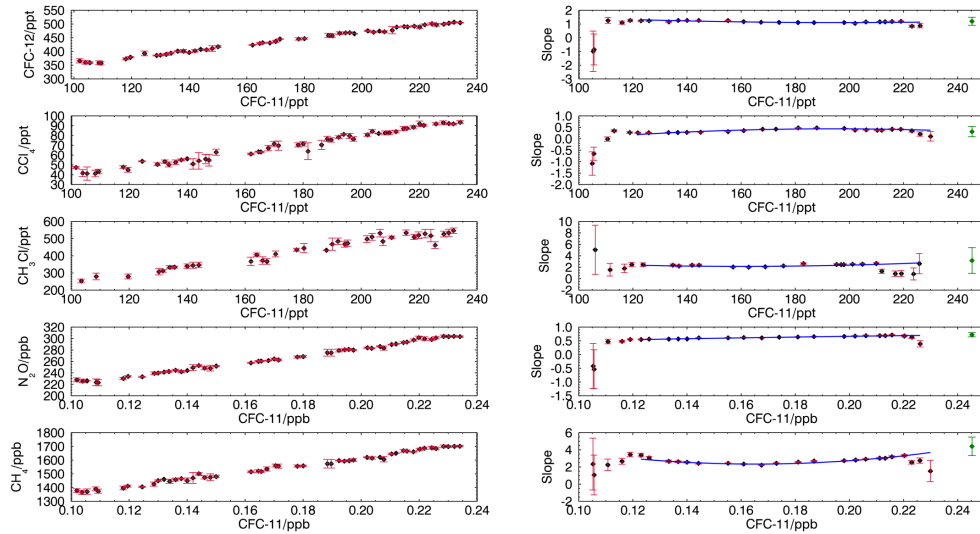
Fig. B16. Correlations between the volume mixing ratios of CFC-12, CCl$_4$, CH$_4$, CH$_3$Cl and N$_2$O and CFC-11 for the data from the Southern Hemisphere during the stratospheric winter of 2005. Panel descriptions as in Fig. B1.
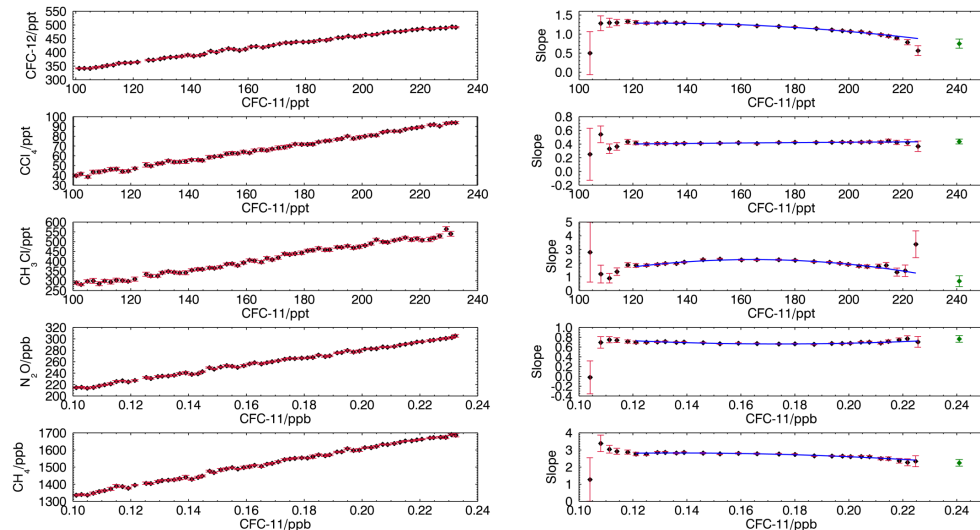
Fig. B17. Correlations between the volume mixing ratios of CFC-12, CCl$_4$, CH$_4$, CH$_3$Cl and N$_2$O and CFC-11 for the data from the Southern Hemisphere during the stratospheric winter of 2006. Panel descriptions as in Fig. B1.
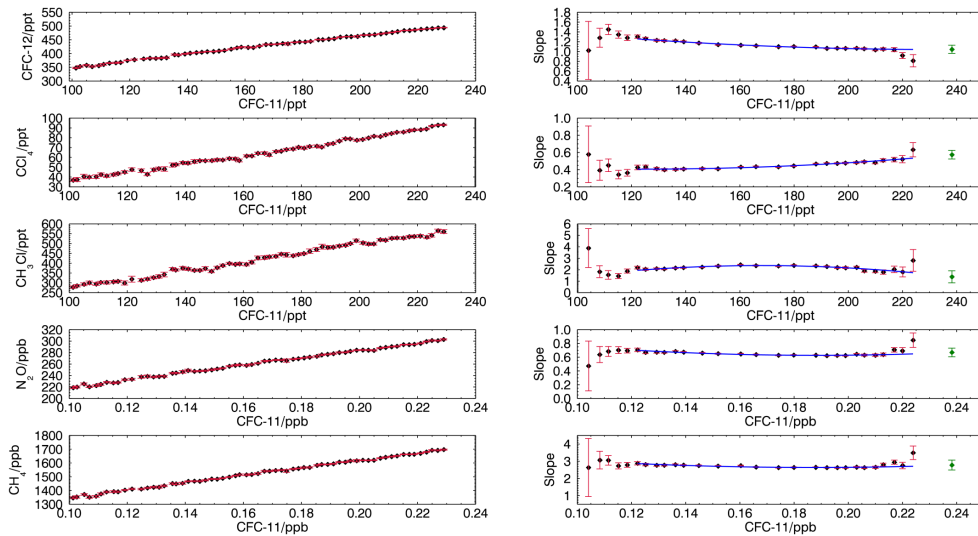
Fig. B18. Correlations between the volume mixing ratios of CFC-12, CCl$_4$, CH$_4$, CH$_3$Cl and N$_2$O and CFC-11 for the data from the Southern Hemisphere during the stratospheric winter of 2007. Panel descriptions as in Fig. B1.
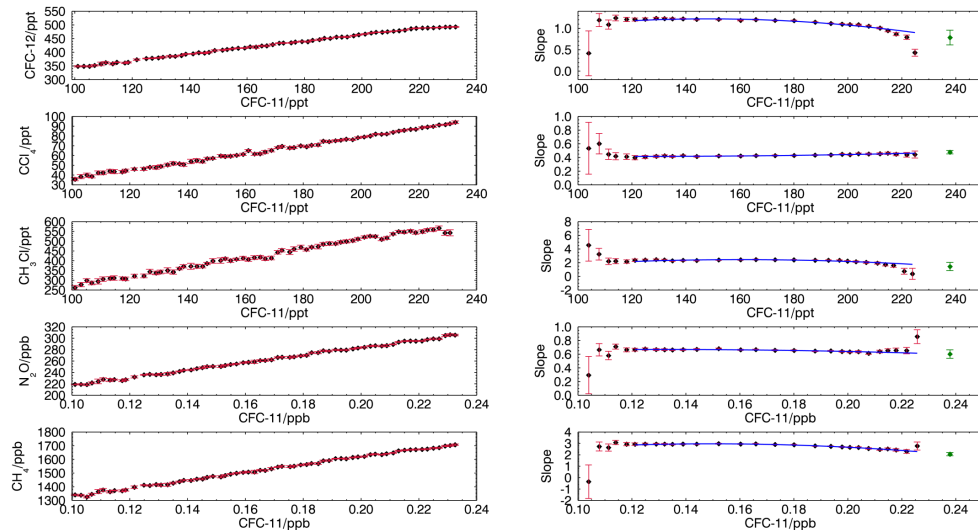
Fig. B19. Correlations between the volume mixing ratios of CFC-12, CCl$_4$, CH$_4$, CH$_3$Cl and N$_2$O and CFC-11 for the data from the Southern Hemisphere during the stratospheric winter of 2008. Panel descriptions as in Fig. B1.
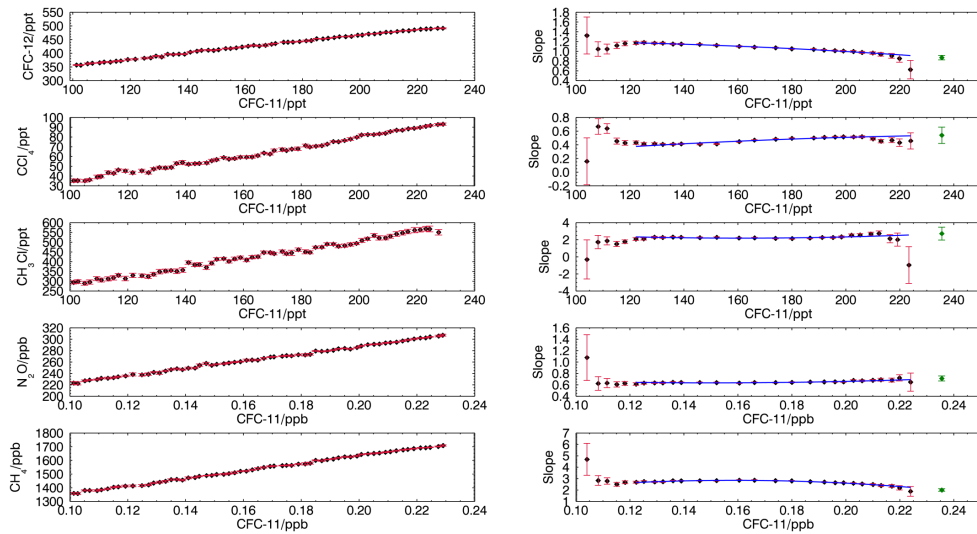
Fig. B20. Correlations between the volume mixing ratios of CFC-12, CCl$_4$, CH$_4$, CH$_3$Cl and N$_2$O and CFC-11 for the data from the Southern Hemisphere during the stratospheric winter of 2009. Panel descriptions as in Fig. B1.
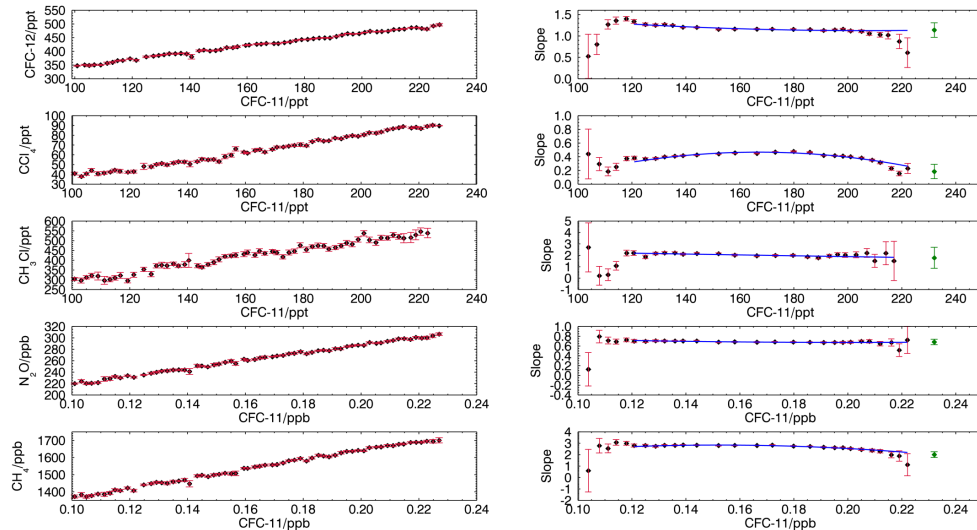
Fig. B21. Correlations between the volume mixing ratios of CFC-12, CCl$_4$, CH$_4$, CH$_3$Cl and N$_2$O and CFC-11 for the data from the Southern Hemisphere during the stratospheric winter of 2010. Panel descriptions as in Fig. B1.

Appendix C

The mean vertical profiles of the species used in this study
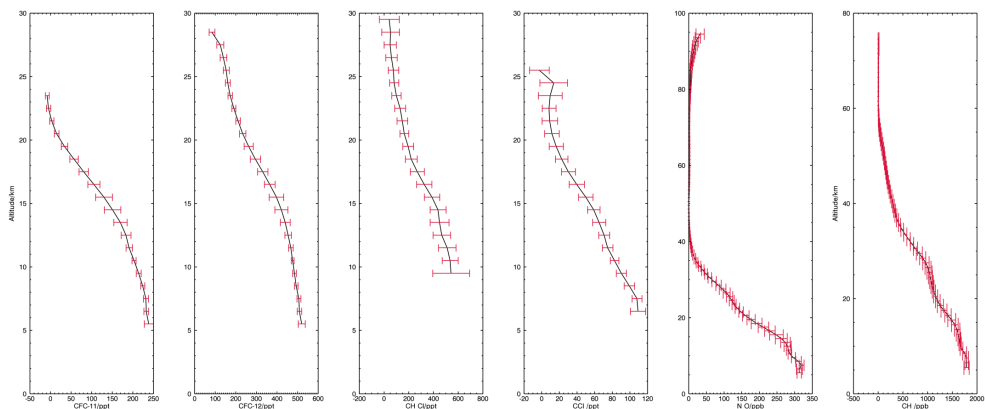
Fig. C2. The mean vertical profile of CFC-11, CFC-12, CH$_3$Cl, CCl$_4$, N$_2$O and CH$_4$, calculated using data from 2009 between 90° and 75° N.
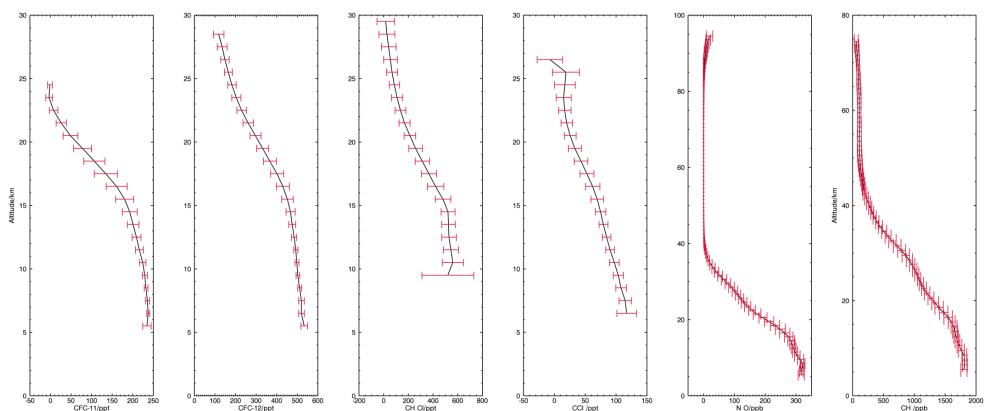
Fig. C3. The mean vertical profile of CFC-11, CFC-12, CH$_3$Cl, CCl$_4$, N$_2$O and CH$_4$, calculated using data from 2009 between 75° and 60° N.
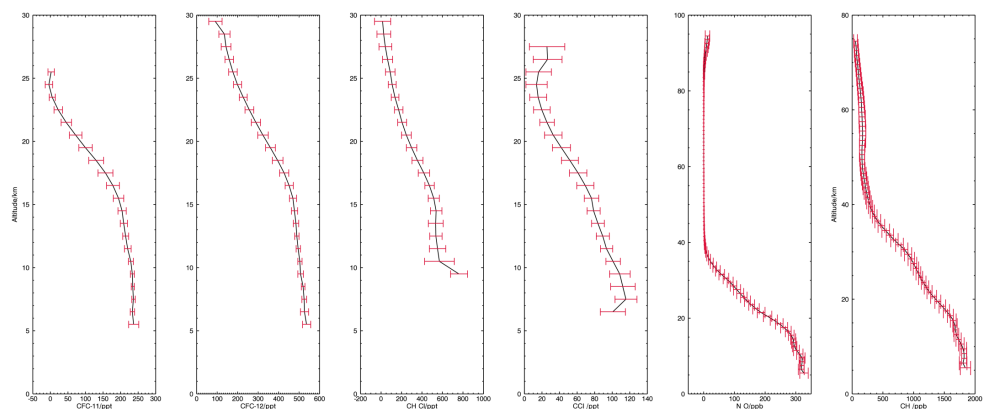
Fig. C4. The mean vertical profile of CFC-11, CFC-12, CH$_3$Cl, CCl$_4$, N$_2$O and CH$_4$, calculated using data from 2009 between 60° and 45° N.
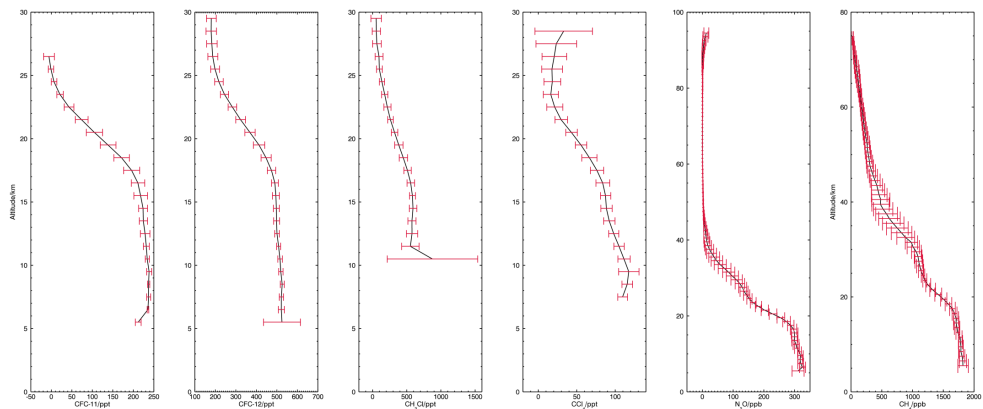
Fig. C5. The mean vertical profile of CFC-11, CFC-12, CH$_3$Cl, CCl$_4$, N$_2$O and CH$_4$, calculated using data from 2009 between 45° and 30° N.
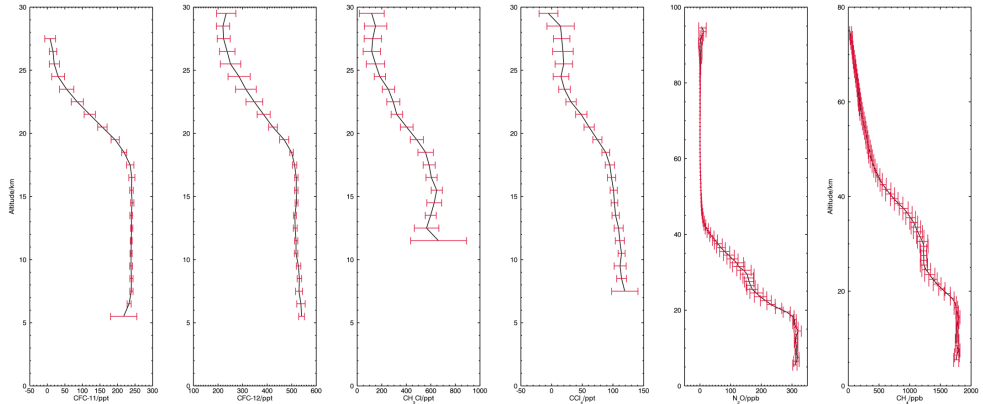
Fig. C6. The mean vertical profile of CFC-11, CFC-12, CH$_3$Cl, CCl$_4$, N$_2$O and CH$_4$, calculated using data from 2009 between 30° and 15° N.
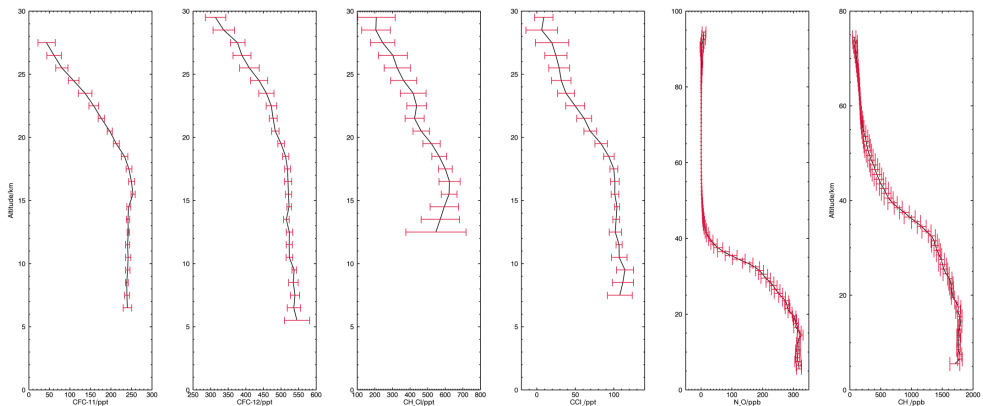
Fig. C7. The mean vertical profile of CFC-11, CFC-12, CH$_3$Cl, CCl$_4$, N$_2$O and CH$_4$, calculated using data from 2009 between 15° and 0° N.
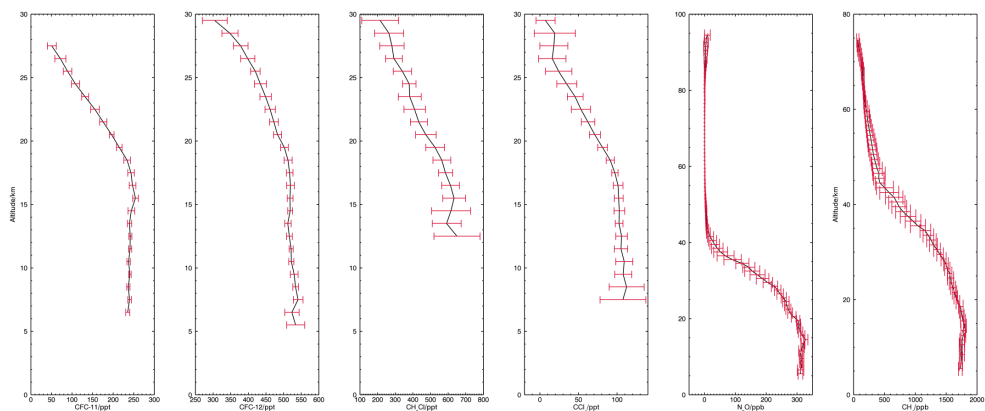
Fig. C8. The mean vertical profile of CFC-11, CFC-12, CH$_3$Cl, CCl$_4$, N$_2$O and CH$_4$, calculated using data from 2009 between 0° and 15° S.
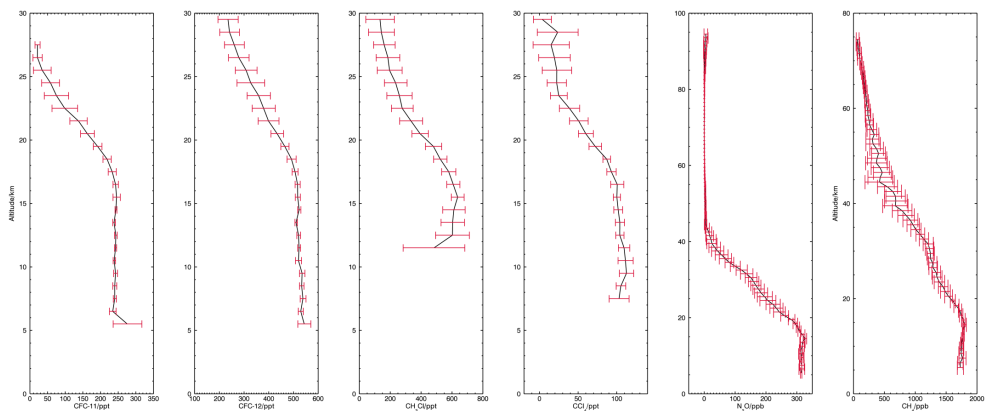
Fig. C9. The mean vertical profile of CFC-11, CFC-12, CH$_3$Cl, CCl$_4$, N$_2$O and CH$_4$, calculated using data from 2009 between 15° and 30° S.
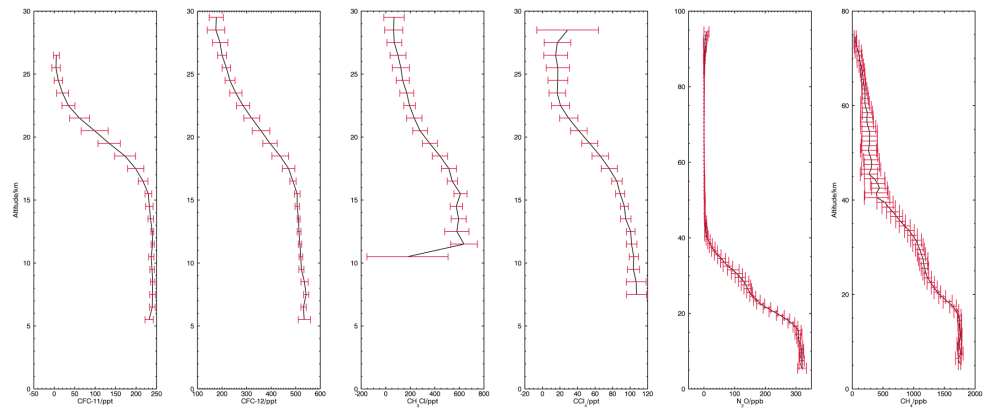
Fig. C10. The mean vertical profile of CFC-11, CFC-12, CH$_3$Cl, CCl$_4$, N$_2$O and CH$_4$, calculated using data from 2009 between 30° and 45° S.
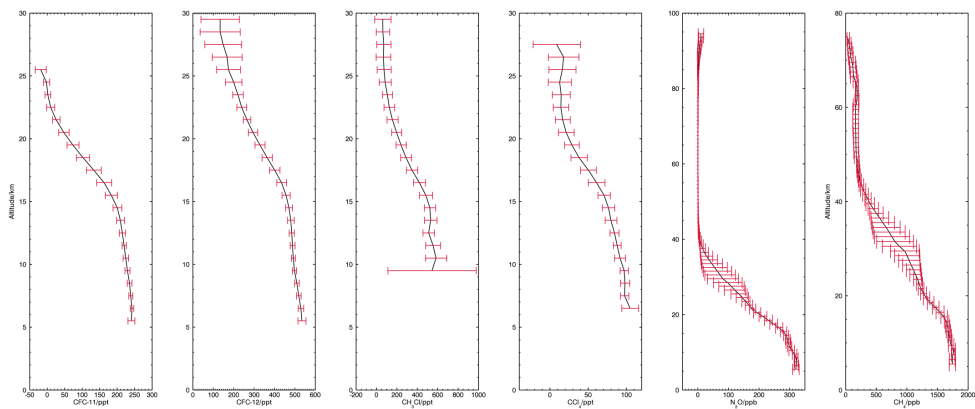
Fig. C11. The mean vertical profile of CFC-11, CFC-12, CH$_3$Cl, CCl$_4$, N$_2$O and CH$_4$, calculated using data from 2009 between 45° and 60° S.
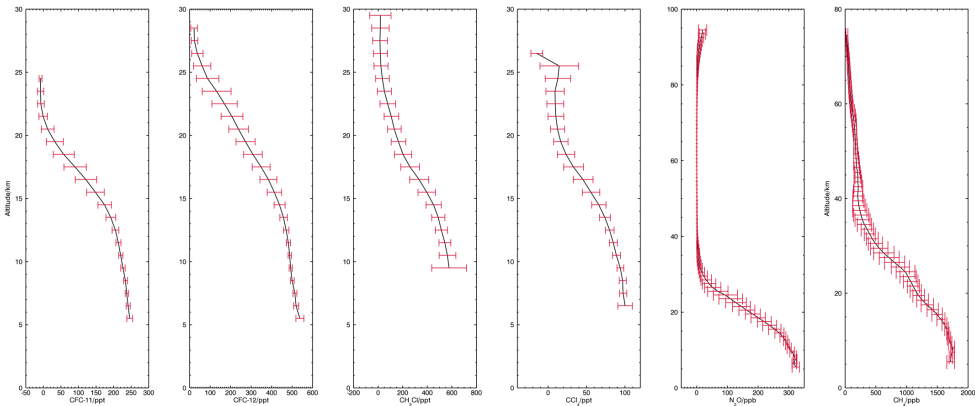
Fig. C12. The mean vertical profile of CFC-11, CFC-12, CH$_3$Cl, CCl$_4$, N$_2$O and CH$_4$, calculated using data from 2009 between 60° and 75° S.
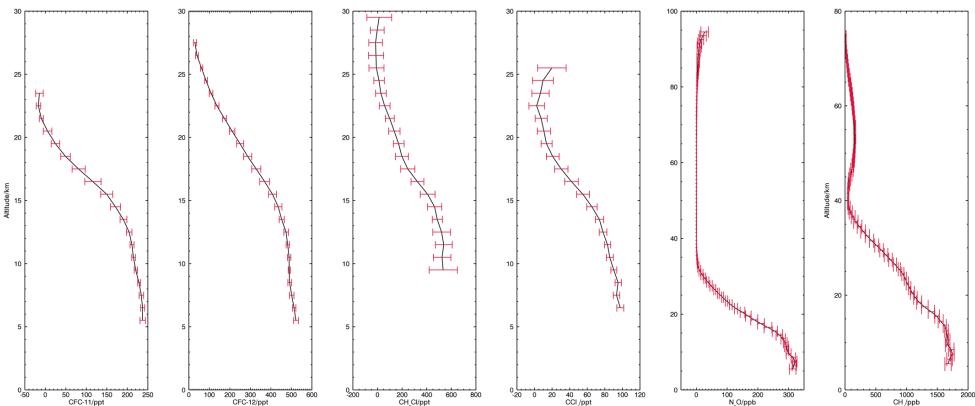
Fig. C13. The mean vertical profile of CFC-11, CFC-12, CH$_3$Cl, CCl$_4$, N$_2$O and CH$_4$, calculated using data from 2009 between 75° and 90° S.

References

Allen, N. D. C., Bernath, P. F., Boone, C. D., Chipperfield, M. P., Fu, D., Manney, G. L., Oram, D. E., Toon, G. C., and Weisenstein, D. K.: Global carbon tetrachloride distributions obtained from the Atmospheric Chemistry Experiment (ACE), Atmos. Chem. Phys., 9, 7449–7459, doi:10.5194/acp-9-7449-2009, 2009.

Bernath, P. F.: Atmospheric chemistry experiment (ACE): Analytical chemistry from orbit, TrAC Trends in Analytical Chemistry, 25, 647–654, doi:10.1016/j.trac.2006.05.001, 2006.

Bernath, P. F., McElroy, C. T., Abrams, M. C., Boone, C. D., Butler, M., Camy-Peyret, C., Carleer, M., Clerbaux, C., Coheur, P. F., Colin, R., DeCola, P., DeMazière, M., Drummond, J. R., Dufour, D., Evans, W. F. J., Fast, H., Fussen, D., Gilbert, K., Jennings, D. E., Llewellyn, E. J., Lowe, R. P., Mahieu, E., McConnell, J. C., McHugh, M., McLeod, S. D., Michaud, R., Midwinter, C., Nassar, R., Nichitiu, F., Nowlan, C., Rinsland, C. P., Rochon, Y. J., Rowlands, N., Semeniuk, K., Simon, P., Skelton, R., Sloan, J. J., Soucy, M. A., Strong, K., Tremblay, P., Turnbull, D., Walker, K. A., Walkty, I., Wardle, D. A., Wehrle, V., Zander, R., and Zou, J.: Atmospheric Chemistry Experiment (ACE): Mission overview, Geophys. Res. Lett., 32, L15S01, doi:10.1029/2005gl022386, 2005.

Boone, C. D., Nassar, R., Walker, K. A., Rochon, Y., McLeod, S. D., Rinsland, C. P., and Bernath, P. F.: Retrievals for the atmospheric chemistry experiment Fourier-transform spectrometer, Appl. Opt., 44, 7218–7231, 2005.

Brown, A. T., Chipperfield, M. P., Boone, C., Wilson, C., Walker, K. A., and Bernath, P. F.: Trends in atmospheric halogen containing gases since 2004, J. Quant. Spectrosc. Ra., 112, 2552–2566, doi:10.1016/j.jqsrt.2011.07.005, 2011.

Bujok, O., Tan, V., Klein, E., Nopper, R., Bauer, R., Engel, A., Gerhards, M.-T., Afchine, A., McKenna, D. S., Schmidt, U., Wienhold, F. G., and Fischer, H.: GHOST – A Novel Airborne Gas Chromatograph for In Situ Measurements of Long-Lived Tracers in the Lower Stratosphere: Method and Applications, J. Atmos. Chem., 39, 37–64, doi:10.1023/a:1010789715871, 2001.

Cox, M. L., Sturrock, G. A., Fraser, P. J., Siems, S. T., Krummel, P. B., and O'Doherty, S.: Regional Sources of Methyl Chloride, Chloroform and Dichloromethane Identified from AGAGE Observations at Cape Grim, Tasmania, 1998–2000, J. Atmos. Chem., 45, 79–99, doi:10.1023/a:1024022320985, 2003.

Cunnold, D. M., Weiss, R. F., Prinn, R. G., Hartley, D., Simmonds, P. G., Fraser, P. J., Miller, B., Alyea, F. N., and Porter, L.: GAGE/AGAGE measurements indicating reductions in global emissions of CCl3F and CCl2F2 in 1992–1994, J. Geophys. Res., 102, 1259–1269, doi:10.1029/96jd02973, 1997.

Cunnold, D. M., Steele, L. P., Fraser, P. J., Simmonds, P. G., Prinn, R. G., Weiss, R. F., Porter, L. W., O'Doherty, S., Langenfelds, R. L., Krummel, P. B., Wang, H. J., Emmons, L., Tie, X. X., and Dlugokencky, E. J.: In situ measurements of atmospheric methane at GAGE/AGAGE sites during 1985–2000 and resulting source inferences, J. Geophys. Res., 107, 4225, doi:10.1029/2001jd001226, 2002.

Douglass, A. R., Stolarski, R. S., Schoeberl, M. R., Jackman, C. H., Gupta, M. L., Newman, P. A., Nielsen, J. E., and Fleming, E. L.: Relationship of loss, mean age of air and the distribution of CFCs to stratospheric circulation and implications for atmospheric lifetimes, J. Geophys. Res., 113, D14309, doi:10.1029/2007jd009575, 2008.

Efron, B.: Bootstrap methods: Another look at the jackknife, Ann. Stat., 7, 1–26, 1979/

Gunson, M. R., Abbas, M. M., Abrams, M. C., Allen, M., Brown, L. R., Brown, T. L., Chang, A. Y., Goldman, A., Irion, F. W., Lowes, L. L., Mahieu, E., Manney, G. L., Michelsen, H. A., Newchurch, M. J., Rinsland, C. P., Salawitch, R. J., Stiller, G. P., Toon, G. C., Yung, Y. L., and Zander, R.: The Atmospheric Trace Molecular Spectroscopy (ATMOS) experiment: Deployment on the ATLAS Space Shuttle Missions, Geophys. Res. Lett., 23, 2333–2336, 1996.

Irion, F. W., Gunson, M. R., Toon, G. C., Chang, A. Y., Eldering, A., Mahieu, E., Manney, G. L., Michelsen, H. A., Moyer, E. J., Newchurch, M. J., Osterman, G. B., Rinsland, C. P., Salawitch, R. J., Sen, B., Yung, Y. L., and Zander, R.: Atmospheric Trace Molecule Spectroscopy (ATMOS) Experiment Version 3 data retrievals, Appl. Opt., 41, 6968–6979, 2002.

Johnston, H. S., Serang, O., and Podolske, J.: Instantaneous Global Nitrous Oxide Photochemical Rates, J. Geophys. Res., 84, 5077–5082, doi:10.1029/JC084iC08p05077, 1979.

Laube, J. C., Keil, A., Bönisch, H., Engel, A., Röckmann, T., Volk, C. M., and Sturges, W. T.: Observation-based assessment of stratospheric fractional release, lifetimes, and ozone depletion potentials of ten important source gases, Atmos. Chem. Phys., 13, 2779–2791, doi:10.5194/acp-13-2779-2013, 2013.

Lide, D.: Handbook of Chemistry and Physics, in, Chemical Rubber Publishing Company, USA, 9–109, 1990.

Mäder, J. A., Staehelin, J., Peter, T., Brunner, D., Rieder, H. E., and Stahel, W. A.: Evidence for the effectiveness of the Montreal Protocol to protect the ozone layer, Atmos. Chem. Phys., 10, 12161–12171, doi:10.5194/acp-10-12161-2010, 2010.

Mahieu, E., Duchatelet, P., Demoulin, P., Walker, K. A., Dupuy, E., Froidevaux, L., Randall, C., Catoire, V., Strong, K., Boone, C. D., Bernath, P. F., Blavier, J.-F., Blumenstock, T., Coffey, M., De Mazière, M., Griffith, D., Hannigan, J., Hase, F., Jones, N., Jucks, K. W., Kagawa, A., Kasai, Y., Mebarki, Y., Mikuteit, S., Nassar, R., Notholt, J., Rinsland, C. P., Robert, C., Schrems, O., Senten, C., Smale, D., Taylor, J., Tétard, C., Toon, G. C., Warneke, T., Wood, S. W., Zander, R., and Servais, C.: Validation of ACE-FTS v2.2 measurements of HCl, HF, CCl3F and CCl2F2 using space-, balloon- and ground-based instrument observations, Atmos. Chem. Phys., 8, 6199–6221, doi:10.5194/acp-8-6199-2008, 2008.

Minschwaner, K., Carver, R. W., Briegleb, B. P., and Roche, A. E.: Infrared radiative forcing and atmospheric lifetimes of trace species based on observations from UARS, J. Geophys. Res., 103, 23243–23253, doi:10.1029/98jd02116, 1998.

Montzka, S. A., Reimann, S., (Coordinating Lead Authors), Engel, A., Krüger, K., O'Doherty, S., Sturges, W. T., Blake, D., Dorf, M., Fraser, P., Froidevaux, L., Jucks, K., Kreher, K., Kurylo, M. J., Mellouki, A., Miller, J., Nielsen, O.-J., Orkin, V. L., Prinn, R.

G., Rhew, R., Santee, M. L., Stohl, A., and Verdonik, D.: Ozone-Depleting Substances (ODSs) and Related Chemicals, Chapter 1 in Scientific Assessment of Ozone Depletion: 2010, Global Ozone Research and Monitoring Project-Report No. 52, World Meteorological Organization, Geneva, Switzerland, 2011.

Neu, J. L and Plumb, R. A.,: Age of air in a "leaky pipe" model of stratospheric transport, J. Geophys. Res., 104, 19243–19255, 1999.

Plumb, R. A.: A tropical pipe model of stratospheric transport, J. Geophys. Res., 101, 3957–3972, doi:10.1029/95jd03002, 1996.

Plumb, R. A.: Stratospheric Transport, Journal of Meteorological Society of Japan, 80, 793–809, 2002.

Plumb, R. A.: Tracer interrelationships in the stratosphere, Rev. Geophys., 45, RG4005, doi:10.1029/2005rg000179, 2007.

Plumb, R. A. and Ko, M. K. W.: Interrelationships between mixing ratios of long-lived stratospheric constituents, J. Geophys. Res., 97, 10145–10156, doi:10.1029/92jd00450, 1992.

Prinn, R., Cunnold, D., Rasmussen, R., Simmonds, P., Alyea, F., Crawford, A., Fraser, P., and Rosen, R.: Atmospheric Emissions and Trends of Nitrous Oxide Deduced From 10 Years of ALE;GAGE Data, J. Geophys. Res., 95, 18369–18385, doi:10.1029/JD095iD11p18369, 1990.

Prinn, R. G., Zander, R., (Coordinating Lead Authors), Cunnold, D. M., Elkins, J. W., Engel, A., Fraser, P. J., Gunson, M. R., Ko, M. K. W., Mahieu, E., Midgley, P. M., Russell III, J. M., Volk, C. M., and Weis, R. F.: Long-Lived Ozone-Related Compounds, Chapter 1 in Scientific Assessment of Ozone Depletion: 1998, Global Ozone Research and Monitoring Project-Report No. 52, World Meteorological Organization, Geneva, Switzerland, 1999.

Prinn, R. G., Weiss, R. F., Fraser, P. J., Simmonds, P. G., Cunnold, D. M., Alyea, F. N., O'Doherty, S., Salameh, P., Miller, B. R., Huang, J., Wang, R. H. J., Hartley, D. E., Harth, C., Steele, L. P., Sturrock, G., Midgley, P. M., and McCulloch, A.: A history of chemically and radiatively important gases in air deduced from ALE/GAGE/AGAGE, J. Geophys. Res., 105, 17751–17792, doi:10.1029/2000jd900141, 2000.

Prinn, R. G., Huang, J., Weiss, R. F., Cunnold, D. M., Fraser, P. J., Simmonds, P. G., McCulloch, A., Harth, C., Salameh, P., O'Doherty, S., Wang, R. H. J., Porter, L., and Miller, B. R.: Evidence for Substantial Variations of Atmospheric Hydroxyl Radicals in the Past Two Decades, Science, 292, 1882–1888, doi:10.1126/science.1058673, 2001.

Rigby, M., Prinn, R. G., Fraser, P. J., Simmonds, P. G., Langenfelds, R. L., Huang, J., Cunnold, D. M., Steele, L. P., Krummel, P. B., Weiss, R. F., O'Doherty, S., Salameh, P. K., Wang, H. J., Harth, C. M., Mühle, J., and Porter, L. W.: Renewed growth of atmospheric methane, Geophys. Res. Lett., 35, L22805, doi:10.1029/2008gl036037, 2008.

Simmonds, P. G., Cunnold, D. M., Weiss, R. F., Prinn, R. G., Fraser, P. J., McCulloch, A., Alyea, F. N., and O'Doherty, S.: Global trends and emission estimates of CCl4 from in situ background observations from July 1978 to June 1996, J. Geophys. Res., 103, 16017–16027, doi:10.1029/98jd01022, 1998.

Simmonds, P., Derwent, R., Manning, A., Fraser, P., Krummel, P., O'Doherty, S., Prinn, R., Cunnold, D., Miller, B., Wang, H., Ryall, D., Porter, L., Weiss, R., and Salameh, P.: AGAGE Observations of Methyl Bromide and Methyl Chloride at Mace Head, Ireland, and Cape Grim, Tasmania, 1998–2001, J. Atmos. Chem., 47, 243–269, doi:10.1023/B:JOCH.0000021136.52340.9c, 2004.

Solomon, S., Qin, D., Manning, M., Alley, R. B., Berntsen, T.,Bindoff, N. L., Chen, Z., Chidthaisong, A., Gregory, J. M., Hegerl, G. C., Heimann, M., Hewitson, B., Hoskins, B. J., Joos, F., Jouzel, J., Kattsov, V., Lohmann, U., Matsuno, T., Molina, M., Nicholls, N., Overpeck, J., Raga, G., Ramaswamy, V., Ren, J., Rusticucci, M., Somerville, R., Stocker, T. F., Whetton, P., Wood, R. A., and Wratt, D: Climate Change 2007: The Physical Science Basis. Contribution of Working Group I to the Fourth Assessment Report of the Intergovernmental Panel on Climate Change, Cambridge University Press, Cambridge, 2007.

Solomon, S., Rosenlof, K. H., Portmann, R. W., Daniel, J. S., Davis, S. M., Sanford, T. J., and Plattner, G. K.: Contribution of stratospheric Water Vapor to Decadal Changes in the Rate of Global Warming, Science, 327, 1219, doi:10.1126/science.1182488, 2010.

UNEP: Handbook for the Montreal Protocol on Substances that Deplete the Ozone Layer 8ed., Secretariat for The Vienna Convention for the Protection of the Ozone Layer & The Montreal Protocol on Substances that Deplete the Ozone Layer, Kenya, 2009.

Velders, G. J. M., Andersen, S. O., Daniel, J. S., Fahey, D. W., and McFarland, M.: The importance of the Montreal Protocol in protecting climate, P. Natl. Acad. Sci., 104, 4814–4819, doi:10.1073/pnas.0610328104, 2007.

Velazco, V. A., Toon, G. C., Blavier, J.-F. L., Kleinböhl, A., Manney, G. L., Daffer, W. H., Bernath, P. F., Walker, K. A., and Boone, C.: Validation of the Atmospheric Chemistry Experiment by noncoincident MkIV balloon profiles, J. Geophys. Res., 116, D06306, doi:10.1029/2010jd014928, 2011.

Volk, C. M., Elkins, J. W., Fahey, D. W., Dutton, G. S., Gilligan, J. M., Loewenstein, M., Podolske, J. R., Chan, K. R., and Gunson, M. R.: Evaluation of source gas lifetimes from stratospheric observations, J. Geophys. Res., 102, 25543–25564, doi:10.1029/97jd02215, 1997.